

ASSET DIVERSIFICATION VERSUS CLIMATE ACTION*

BY CHRISTOPH HAMBEL, HOLGER KRAFT, AND FREDERICK VAN DER PLOEG

Tilburg University, The Netherlands; Goethe University, Germany; University of Oxford, U.K.

Asset pricing and climate policy are analyzed in a global economy where consumption goods are produced by both a green and a carbon-intensive sector. Given that the economy is initially heavily dependent on carbon-intensive capital, the desire to diversify assets complements the attempt to mitigate economic damages from climate change. In the longer run, however, a trade-off between diversification and climate action emerges. We derive the optimal carbon price and the equilibrium risk-free rate, and risk premia. Climate disasters significantly decrease the risk-free rate but increase risk premia on financial assets, especially if no climate policy is implemented.

1. INTRODUCTION

Climate change impacts all areas of human life and impacts economic activity.¹ To avoid carbon-dioxide emissions and climate change, emissions-free technologies and renewable energies are developed. Depending on the perceived severity of the consequences of climate change, there are different opinions about how urgent it is to transition to a less carbon-intensive or carbon-free economy. We are interested in the interplay between financial considerations and policies to mitigate climate change and answer three key policy questions. First, does the financial need to diversify assets hamper or help the fight against climate change and how does it affect optimal carbon pricing? Second, how does climate change and the desire to combat it affect the risk-free interest rate and precautionary saving? We highlight that there is a subtle dynamic interdependence between the financial goal to diversify assets in portfolios and the environmental goal to reduce carbon emissions. Third, we allow for a falling cost of renewables driven by learning by doing (LBD) during the green transition, and examine whether the key insights still hold.

*Manuscript received September 2022; revised November 2023.

We thank Daniel Andrei, Patrick Bolton, Julia Braun, Jesus Fernandez-Villaverde (the editor), Ruediger Kiesel, Thomas Lontzek, Colin Mayer, Stavros Panageas, Armon Rezai, Suphi Sen, Eduardo Schwartz, Gerhard Stahl, Christian Traeger, Frank Venmans, and the participants of the Finance seminar at McGill, seminars at Humboldt University, the University of Lausanne, EARES, University of Brussels, Paris School of Economics, University of Western Australia, the Banca d'España, the Bundesbank and de Nederlandsche Bank, the European Finance Association (EFA) Meeting 2020, the European Economics Association (EEA) Meeting 2020, the SURED Meeting 2020, the EAERE Meeting 2020, the EBI Global Annual Conference 2020, the German Finance Association Meeting 2021, and the Verein fuer Sozialpolitik (VfS) Meeting 2021, the DEARE Meeting 2023, the DVfVM meeting 2023, as well as three anonymous referees for very helpful comments and suggestions. All remaining errors are our own. Christoph Hambel and Holger Kraft gratefully acknowledge financial support by the Deutsche Forschungsgemeinschaft (DFG). Please address correspondence to: Christoph Hambel, Tilburg University, Department of Econometrics and Operations Research, P.O.box 90153, 5000 LE Tilburg, The Netherlands. Phone: +31 (0) 13 466 8908. E-mail: c.hambel@tilburguniversity.edu.

* Van der Ploeg is also affiliated with the University of Amsterdam, CEPR, and CESifo.

¹ See, for example, Scheffers et al. (2019).

Our economic framework is a stochastic macroeconomic growth model with two capital stocks and two energy sources. The green sector takes carbon-free or green energy as input. The brown sector is carbon-intensive and requires fossil fuel whose combustion leads to carbon emissions. Although our contribution is more methodological than empirical, the brown sector includes coal-fired power stations, steel, cement, aluminum, fossil-based transport (including sea- and airports), and the oil, gas, and coal sectors. The green sector includes the sectors that do not depend excessively on oil, gas, or coal but depend on solar or wind energy.

There are two types of capital stocks, brown and green. Investments and capital reallocation from the brown to the green capital stock are both subject to intertemporal and intersectoral adjustment costs. Capital stock accumulation is exposed to diffusive shocks as well as the risk of macroeconomic disasters. We have a two-sector endogenous growth (AK) model and abstract from directed technical change toward green technologies in the spirit of Bovenberg and Smulders (1996), Acemoglu et al. (2012), and Casey (2024), but we do allow for LBD in only the production of the green good which thus captures some features of directed technical change. Emissions are proportional to fossil fuel use and temperature is driven by cumulative emissions.² We allow for two effects of climate change on economic activity: the standard one is that higher temperature leads to a higher share of damages in predamage output as in the seminal DICE-2016R2 model (e.g., Nordhaus 2017); the novel one is that higher temperatures increase the Poisson risk of climate-related disasters (cf. Bansal et al., 2019; Karydas and Xepapadeas, 2022).

We first analyze the interplay between the intensity of climate action proxied by the carbon price and the economic motive to diversify. Given that the economy is initially dominated by the brown capital stock, there are two complementary goals. The first is to mitigate climate change by decarbonizing the economy. The second is to diversify the economy. Both goals require decision makers to initially reduce the brown capital stock. The speed of transition toward a low-carbon economy is thus initially amplified by the diversification motive. Over time, however, the two goals start to conflict. From a diversification perspective, the process should be stopped if there is a balance between green and brown capital. But from an environmental perspective the brown capital stock should eventually be run down completely. Our various calibrations show, however, that this does not occur unless damages from global warming are extremely severe relative to those in the DICE model of Nordhaus (2017). Effectively, climate policy drives the brown capital stock below the fully diversified level; diversification considerations may prevent policymakers from driving it to zero.

Second, we investigate the interplay between climate change and asset prices. We focus on the risk-free rate and the precautionary savings motive during the transition from a carbon-intensive toward a low- or zero-emissions economy. To separate economic from climate effects, our model includes the risk of macroeconomic disaster shocks as in Barro (2006, 2009) and Pindyck and Wang (2013). Hence, our model can generate the high equity premium and low risk-free rate observed in historical data even if climate change has no significant impact on the economy. Taking the effects of climate change into account, we find that the risk-free interest rate decreases in response to rising temperatures reflecting the additional precautionary savings needed to cope with global warming.³

Third, we allow for falling costs of renewable energy as a result of LBD (also known as Swanson's or Wright's law). This requires both a carbon tax to internalize the global warming externalities and a renewable energy subsidy to internalize the LBD externalities. The green transition now occurs more quickly, but the diversification objectives frustrating the latter phases of the green transition still show up.

² See Matthews et al. (2009), Allen et al. (2009), IPCC (2014), van der Ploeg (2018), and Dietz and Venmans (2019), among others, for further references.

³ Risk premia are only significantly affected if we allow for potential climate disasters for which the probability of them occurring increases with temperature. Then, the risk premia increase with higher temperature. Without such temperature-dependent disasters, this effect is modest.

Our integrated assessment model (IAM) enriches an asset pricing framework with rare macroeconomic disasters as in Barro (2006, 2009) or Wachter (2013) by adding the climate module of an IAM. Our representative agent has recursive utility as in Bansal and Yaron (2004) and Pindyck and Wang (2013). If the sizes of the two sectors would be exogenous and the effect of climate change is disregarded, the two-tree model analyzed in Cochrane et al. (2007) arises as a special case. In our IAM, we have a stochastic two-sector growth model with temperature driven by cumulative emissions.

Our two-sector IAM thus differs from one-sector IAMs which do not focus on asset pricing. For example, the DICE model has one sector and is widely used to study optimal carbon abatement and carbon pricing. It combines a Ramsey-type model for capital allocation with deterministic dynamics of the economy, emissions, carbon dioxide, and global temperature (e.g., Nordhaus 1992, 2017). Crost and Traeger (2014), Jensen and Traeger (2014), Ackerman et al. (2013), Bretschger and Vinogradova (2019), van den Bremer and van der Ploeg (2021), Hambel et al. (2021a), and Lemoine (2021) use recursive utility to analyze stochastic models of the economy and the climate. Cai and Lontzek (2019) extend the DICE model with stochastic growth and the risk of tipping points. Golosov et al. (2014) obtain closed-form solutions in a one-sector framework with log utility, Cobb–Douglas production, full depreciation in one discrete time period, and damages that are an exponential function of the atmospheric carbon stock. Traeger (2023) generalizes this setting to recursive preferences and provides a description of the carbon cycle and the climate system. He also allows for epistemological uncertainty and anticipated learning.

Few papers combine asset pricing with an IAM.⁴ Barnett et al. (2020) analyze a stochastic one-sector macroeconomic dynamic stochastic general equilibrium (DSGE) model with stochastic economic growth rates and endogenous investments in fossil fuel reserves. They also address preference-based concerns about ambiguity and model misspecification. Barnett (2023a) uses an extended Fama–French three-factor model to estimate negative effects of temperature on excess returns for brown portfolios and positive effects for green portfolios. He also derives optimal climate policy from a two-sector DSGE model. Whereas this study in contrast to our analysis allows for model uncertainty, we allow for macroeconomic and climatic disasters.

Bansal et al. (2017, 2019) quantify the impact of local temperature on asset prices. They study a global long-run risk model that simultaneously matches the observed temperature and consumption growth dynamics. Furthermore, their model can generate a low risk-free interest rate and a high equity premium (cf. Donadelli et al., 2017). Karydas and Xepapadeas (2022) study an economy with two assets, but focus on a Lucas-tree endowment economy where the agent cannot actively control the transition to a low-carbon economy. Finally, Daniel et al. (2019) show in an asset pricing setting that recursive preferences with general resolution of uncertainty about climate change can lead to a declining carbon price.⁵

Section 2 introduces our IAM. Section 3 characterizes the social optimum and discusses how the social optimum can be decentralized in the market economy. Section 4 discusses the diversification motive. Section 5 discusses our calibration strategy. Section 6 presents our results on the relation between the diversification motive and climate action. Section 7 discusses how climate change affects the equilibrium risk-free rate, the precautionary savings motive, and risk premia. Section 8 concludes. The appendices give proofs, calibration details, and results on risk premia.⁶

⁴ van den Bremer and van der Ploeg (2021) study a one-sector production economy with endogenous climate change and a wide range of economic and climatic uncertainties that generates low risk-adjusted interest rates and a high risk premium. Like Lemoine (2021), they find that the effect of covariance between climate shocks and economy shocks depends on whether the coefficient of relative risk aversion exceeds one or not. Dietz et al. (2018) define the “climate beta” to be the elasticity of damages with respect to economy activity and show that the optimal carbon price increases in this beta.

⁵ The feature of a declining carbon price is derived from a binomial tree with a fixed horizon.

⁶ For additional material such as the solution approach and a battery of robustness checks, see <http://christoph-hambel.de/wp-content/uploads/2024/01/HKvdP-IER-2024-Online-Appendix.pdf>

2. A TWO-SECTOR MODEL OF THE ECONOMY AND THE CLIMATE

We present a dynamic two-sector AK economy. The green sector uses carbon-free energy as input; the brown (carbon-emitting) sector deploys fossil fuel leading to emissions, warming, and damages to aggregate output.⁷ Temperature depends on cumulative carbon emissions. Energy inputs are available at a cost. The economy can reallocate capital from the brown to the green capital stock which is also costly. Households have recursive preferences so that risk aversion can be disentangled from the elasticity of intertemporal substitution (EIS).

2.1. Production of Goods. Final goods are produced by two sectors. The capital stocks are broad measures that aggregate physical capital, human capital, and nontangible capital such as patents. Outputs of both sectors follow from the Cobb–Douglas production functions

$$Y_n = A_n K_n^{1-\eta_n} F_n^{\eta_n} \Lambda_n(T), \quad n \in \{1, 2\},$$

where K_n is the capital stock of sector n . The rate of energy use in sector n is denoted by F_n where we refer to F_1 as *green energy* and to F_2 as *brown energy* or fossil fuel use. The Cobb–Douglas weight η_n and total factor productivity (TFP) A_n are nonnegative, sector-specific constants. Here, T denotes global average temperature relative to the beginning of the industrial revolution, so $T = 0$ is the pre-industrial level of temperature. The function Λ_n is a sector-specific damage function and shows how much output is curbed in response to higher temperatures (e.g., Nordhaus and Sztorc, 2013). This is the *first channel* by which global warming affects economic activity. We assume that the final goods are perfect substitutes.⁸

2.2. Investments in Green and Brown Capital. Let $I_n \geq 0$ be the investment rate in sector n and $R \geq 0$ the rate at which brown capital is converted into green capital.⁹ Investment is subject to quadratic intertemporal adjustment costs. To convert brown into green capital, the green sector incurs quadratic intrasectoral adjustment costs. A dollar of brown capital is thus converted into less than a dollar of green capital and the wedge increases in the amount converted. Depreciation rates of the capital stocks are $\delta_n^k \geq 0$, $n \in \{1, 2\}$. Capital stock dynamics of the green and brown sector are thus¹⁰

$$(1) \quad dK_1 = \left(I_1 - \frac{1}{2}\phi_1 \frac{I_1^2}{K_1} + R - \frac{1}{2}\kappa \frac{R^2}{K_1} - \delta_1^k K_1 \right) dt + K_1 \sigma_1 dW_1 - K_{1-} (\ell_e dN_e + \ell_c dN_c),$$

$$(2) \quad dK_2 = \left(I_2 - \frac{1}{2}\phi_2 \frac{I_2^2}{K_2} - R - \delta_2^k K_2 \right) dt + K_2 \sigma_2 \left(\rho_{12} dW_1 + \sqrt{1 - \rho_{12}^2} dW_2 \right) - K_{2-} (\ell_e dN_e + \ell_c dN_c),$$

where ϕ_n , $n = 1, 2$, are the investment adjustment cost parameters, κ is the capital reallocation cost parameter, and W_1 and W_2 are two independent Brownian motions. The parameter

⁷ We abstract from financial intermediaries who issue stocks and pay dividends to households. In the absence of borrowing and/or collateral constraints and bankruptcies, this will not affect our results.

⁸ Subsection E.8 of the online appendix relaxes the assumption of perfect substitutes and allows for imperfect substitution between green and brown goods. We then interpret Y_n as intermediate goods that are aggregated into a final good $Y = (Y_1^\rho + Y_2^\rho)^{1/\rho}$ with $\rho \in (0, 1]$ determining the constant elasticity of substitution (CES) between the two sectors. We also adopt a setting where aggregate consumption is a CES-aggregate consisting of the two consumption goods produced in each sector. These extensions do not significantly affect our main results. This specification of the economic structure is rudimentary since there may be a third capital stock which is complementary to the other two capital stocks, say when modeling transport and the power industry, separately.

⁹ The constraint $R \geq 0$ implies that conversion is only feasible from the brown into the green capital stock. We choose the conversion to be one way since we analyze the optimal transition to a carbon-free economy. If we allow for two-way reallocation, the optimal plan is almost never to convert from green into brown capital (results available upon request).

¹⁰ For notational convenience, we drop the time index t if it does not create confusion. Furthermore, K_{n-} is short for $K_{n,t-}$, that is, for the left limit of K_n at time t . For the dt and dW terms, this distinction is irrelevant since the point process N only jumps at countably many time points and Lebesgue and Brownian integrands can be changed at countably many points.

ρ_{12} denotes the instantaneous correlation coefficient between the Brownian shocks of the two capital stocks. N_e and N_c are two independent point process capturing economic and climate disaster risk. Since these disaster shocks are identical for both types of capital in realization, not just in distribution, they significantly increase the total correlation between the two capital stocks.¹¹

The process N_e models macroeconomic disasters whose jump intensity λ_e is constant as in Barro (2006, 2009) and Barro and Jin (2011). The process N_c models climate disasters as in Karydas and Xepapadeas (2022). This is the *second channel* by which global warming curbs economy. Its jump intensity $\lambda_c = \lambda_c(T)$ depends on current temperature T . In both cases, $\lambda_i dt$ is the probability for a jump to occur over the small time interval dt and $1/\lambda_i$ is the expected waiting time to the next jump, $i \in \{e, c\}$. The parameters ℓ_e and ℓ_c are the corresponding jump sizes which are stochastic, but independent of the Brownian and Poisson shocks. We suppose that jump sizes are the same for both types of capital.

Climate damages thus affect the economy via the damage functions $\Lambda_n(T)$ scaling down output in response to climate change as in the DICE model and via the disaster probability increasing in temperature as in Bansal et al. (2019) and Karydas and Xepapadeas (2022). We assume that the size of climate-related disasters does not increase with global warming.

2.3. Emissions and Temperature. Following Allen et al. (2009), Matthews et al. (2009), and IPCC (2014), we let global average temperature T increase linearly in cumulative emissions $E_t = \int_0^t \epsilon_s ds$ measured in gigatons of carbon (GtCs). Global mean temperature is thus

$$T_t = T_0 + \vartheta E_t + \int_0^t \sigma_T dW_{3s},$$

where T_0 is current temperature and ϑ denotes the transient climate response to cumulative emissions (TCRE).¹² W_3 denotes a third standard Wiener process that is independent of W_1 and W_2 and has a constant diffusion coefficient σ_T . Current emissions are $\epsilon = \nu F_2$ where F_2 is the rate of fossil use in energy units and $\nu = \nu(t, T, K_1, K_2)$ the emission intensity per unit of fossil fuel, which may depend on the current state of the world. Hence, we have

$$(3) \quad dT = \beta F_2 dt + \sigma_T dW_3,$$

where $\beta = \vartheta \nu$ and thus β depends on $t, T, K_1,$ and K_2 . Note that $\epsilon = 0$ if $K_2 = 0$, so carbon emissions cease once the brown capital stock has been fully phased out.

2.4. Consumption and Preferences. The consumption good in each sector is the cash-flow net of investments and energy costs,

$$C_n = Y_n - I_n - \frac{b_n(F_n/K_n)^{1/\varepsilon_n}}{1 + 1/\varepsilon_n} F_n,$$

¹¹ Geometric Brownian shocks to the capital stock have been commonly used in the literature for AK models like ours. Following Pindyck and Wang (2013) and Barro (2006, 2009), among others, it is common in continuous-time models to put the geometric Brownian shocks and disaster shocks into the capital dynamics. These shocks are the typical stochastic drivers of total factor productivity and depreciation and thus of economic growth and of asset returns. Since, in contrast to these papers, we study a two-sector model, those shocks represent correlated sectoral level shocks. Hence, total correlation between the two sectors involves instantaneous correlation from geometric Brownian shocks and common jump risk (see Subsection 5.1).

¹² In our model, fossil fuel is not an exhaustible resource. Golosov et al. (2014) do have exhaustible oil with zero extraction costs alongside coal and green energy, but oil plays hardly a role in combating global warming as policy-makers can only affect *when* to extract oil and not *how much* of reserves to extract. To test whether exhaustibility matters for our policy simulations, we have studied a variant of our model that takes account of the following constraint: $E_t \leq \bar{E}$, where \bar{E} denotes the maximum amount of total carbon emissions if all fossil fuel resources were to be exploited. We find that this constraint is not binding if \bar{E} is set in line with recent estimates on exhaustible fossil fuel resources, 11, 000GtCO₂ or 3, 000GtC (McGlade and Ekins, 2015).

where b_1 and b_2 are cost parameters for green energy and fossil fuel and ε_n is the price elasticity of supply in sector n .¹³ The representative household has recursive preferences and consumes $C = C_1 + C_2$. As shown in Duffie and Epstein (1992b), these preferences are the continuous-time version of discrete-time recursive utility developed in Kreps and Porteus (1978) and Epstein and Zin (1989). The value function J is recursively defined by

$$(4) \quad J(t, K_1, K_2, T) = \sup_{I_1, I_2, R, F_1, F_2} \mathbb{E}_t \left[\int_t^\infty f(C_s, J(s, K_{1s}, K_{2s}, T_s)) ds \right],$$

where the aggregator function f is defined by

$$f(C, J) = \begin{cases} \delta \theta J \left[\frac{C^{1-1/\psi}}{[(1-\gamma)J]^{1/\theta}} - 1 \right], & \psi \neq 1, \\ \delta(1-\gamma)J \log \left(\frac{C}{[(1-\gamma)J]^{1-\gamma}} \right), & \psi = 1, \end{cases}$$

where $\theta = \frac{1-\gamma}{1-1/\psi}$, C denotes consumption, γ the coefficient of relative risk aversion, ψ the EIS, and δ the rate of time impatience. The degree of risk aversion γ typically exceeds $1/\psi$ to reflect a preference for early resolution of uncertainty. If risk aversion equals the inverse of the EIS ($\gamma = 1/\psi$ or, equivalently, $\theta = 1$), the preference structure collapses to the more commonly used time-additive constant relative risk-aversion (CRRA) utility.

3. OPTIMALITY CONDITIONS AND THE SOCIAL COST OF CARBON

Following Duffie and Epstein (1992b), the value function $J = J(t, K_1, K_2, T)$ satisfies the Hamilton–Jacobi–Bellman (HJB) equation (A.1). The first-order optimality conditions give rise to efficiency conditions (5)–(8). Optimal investment in sector $n \in \{1, 2\}$ reads

$$(5) \quad I_n = \frac{K_n q_n - 1}{\phi_n q_n}.$$

The higher ϕ_n , the higher adjustment costs and the less the sensitivity of the investment rate to the marginal value of investment. Here, Tobin’s Q of sector n is

$$(6) \quad q_n = \frac{C^{1/\psi}}{\delta} \frac{J_{K_n}}{[(1-\gamma)J]^{1-1/\theta}}.$$

Condition (5) shows that the investment rate in sector n is small if intertemporal adjustment costs are high and large if the sectoral Tobin’s Q is high, where the latter is the marginal value of capital in utility units (i.e., J_{K_n}) divided by the marginal utility of consumption (i.e., $f_C(C, J)$) to obtain the marginal value of capital in units of consumption or final goods. The sectoral Tobin’s Q, the ratio between the market value and the replacement cost of physical capital, is bigger than one, since installing capital is costly and installed capital earns a rent. The optimal reallocation from brown to green capital follows from

$$(7) \quad R = \frac{K_1 q_1 - q_2}{\kappa q_1}.$$

If the marginal value of investments in the green sector exceeds those in the brown sector (i.e., the Tobin’s Q for the green sector exceeds the one for the brown sector), it is optimal

¹³ To keep the model simple, we let the b_n be constant. This assumption can be relaxed in several dimensions, for example, deterministic trends or stochastic shocks to energy prices. By contrast, van den Bremer and van der Ploeg (2021) assume that energy costs remain constant over time, that is, they consider the special case $\varepsilon_n \rightarrow \infty$. Alternative cost specifications do not qualitatively alter our results and are available upon request. Subsection 6.3 gives details of how our analysis is affected if the cost of green goods falls due to LBD.

to reallocate capital from the brown to the green sector. The extent to which this is done increases in the gap between the Tobin's Q's and decreases in the intrasectoral adjustment cost parameter κ , so the conversion rate is small if intratemporal adjustment costs are high.

The optimal use of green energy and fossil fuel follow from

$$(8) \quad \eta_1 A_1 \left(\frac{F_1}{K_1} \right)^{\eta_1 - 1} \Lambda_1(T) = b_1 \left(\frac{F_1}{K_1} \right)^{1/\varepsilon_1}, \quad \eta_2 A_2 \left(\frac{F_2}{K_2} \right)^{\eta_2 - 1} \Lambda_2(T) = b_2 \left(\frac{F_2}{K_2} \right)^{1/\varepsilon_2} + \tau_c \nu,$$

where the social cost of burning one ton of carbon or the SCC is

$$(9) \quad \tau_c = \frac{\tau_f}{\nu} = - \frac{\partial J_T C^{1/\psi}}{\delta[(1-\gamma)J]^{1-1/\theta}}$$

and ν is the emission intensity per unit of fossil fuel (see Subsection 2.3). The marginal product of the green capital stock thus equals the marginal cost of one unit of green energy whereas the marginal product of brown capital equals its marginal cost plus the external effects of emitting carbon. The optimal SCC increases in consumption as marginal damages are proportional to aggregate economic activity (cf. Nordhaus, 1991; Golosov et al., 2014; Rezai and van der Ploeg, 2016; Hambel et al., 2021b). We consider two scenarios. In the *optimal* scenario, the social planner takes account of the SCC (9) and actively reallocates capital from the brown to the green sector (7). In the *business-as-usual* (BAU) scenario, the SCC is not internalized and capital is not actively shifted from the brown to the green sector.¹⁴

We denote the total stock of capital by $K = K_1 + K_2$, so the share of brown to total capital $S = \frac{K_2}{K_1 + K_2}$ defines the carbon-intensity of the economy. During the energy transition, the share of brown capital S decreases over time. Appendix A.1 shows that the value function J , the optimal carbon tax τ_c , and the optimal controls can be reformulated in terms T and S instead of T , K_1 , and K_2 (see Proposition A.1). This simplifies our numerical solution (see Online Appendix B.1), since now there are only two instead of three state variables. It is not feasible to analytically characterize how the SCC depends on S and T , but we will do this numerically.

To replicate the social optimum in the decentralized market economy, we must price carbon, either via a global carbon tax or via a global cap-and-trade system, at a price equal to the optimal SCC. The revenue of the carbon tax or permits is refunded in lump-sum fashion to the private sector. The carbon price thus internalizes the global warming externalities.

4. DIVERSIFICATION MOTIVE

While the quantification of diversification goes back to Markowitz (1952), there is empirical evidence for diversification benefits from green assets in an investor's portfolio indicating that diversification is a relevant consideration when thinking about the green transition. Reboredo (2018), Reboredo and Ugolini (2020), Kuang (2021a, 2021b), among others, show that green assets have considerable diversification effects on stocks, especially on brown energy stocks. Similarly, El Ghouli et al. (2023) show that socially responsible investing offers diversification benefits for mutual funds. We now discuss diversification benefits in our model.

Since damages resulting from climate change increase in temperature, the indirect utility function J decreases in temperature, $\frac{\partial J}{\partial T} < 0$. By contrast, the effect of the share of brown capital on indirect utility is nonmonotone. As S measures how *carbon-intensive* the economy is, a higher value of S indicates that there are more carbon-dioxide emissions amplifying climate change. This argument suggests that J decreases in S . However, the share of brown capital also determines how *diversified* the economy is.

The volatility of the total stock of capital K is a convex function of S . More precisely, the total capital volatility $\|\sigma_k(S)\|$ equals σ_1 and σ_2 at the polar cases, $S = 0$ and $S = 1$, respectively,

¹⁴ Note that the SCC in the BAU scenario exceeds the SCC in the optimal scenario.

but takes its minimum value at

$$(10) \quad S^* = \frac{\sigma_1^2 - \sigma_1\sigma_2\rho_{12}}{\sigma_1^2 + \sigma_2^2 - 2\sigma_1\sigma_2\rho_{12}}.$$

By contrast, for high *and* low values of S the economy is poorly diversified. Since initially brown capital dominates the capital stock, the diversification motive accelerates climate action until the optimal level of diversification is reached. At this level, abatement and diversification become conflicting targets and the transition to a low-carbon economy is thus slowed down. Nevertheless, the economy does not stop at the optimal diversification level and the overall optimal level of S lies below S^* , that is, below the optimal level without externalities. If both capital stocks are equally volatile, $\sigma_1 = \sigma_2$, total capital volatility takes its minimum at $S^* = 1/2$, that is, if both capital stocks are of the same size. We emphasize that then the optimal level of diversification is independent of the instantaneous correlation ρ_{12} .

We emphasize that green and brown asset returns are not uncorrelated in our model. Even without disasters and climate change, zero correlation between Brownian shocks does not imply that asset returns are uncorrelated, see the discussion in Cochrane et al. (2007). The resulting positive correlation between both assets comes from the share of brown capital S , which is a common factor for both assets. In our case, temperature is a second common factor that also affects both capital stocks and, in turn, asset returns. Besides both assets are driven by common macroeconomic disasters. This implies a much higher correlation between the two assets than indicated by the value of ρ_{12} . We illustrate the total correlation for several sample paths in Figure A.6 in the online appendix.

To assess the benefits from diversification, we compare the indirect utility in two scenarios. First, we consider the scenario without diversification, characterized by $\rho_{12} = 1$, and denote the value function in this scenario case by J^* . Second, we consider the benchmark scenario where both capital stocks are not perfectly correlated and the effects of diversification are immanent and denote the value function by J . If diversification has a positive effect, the value functions should satisfy $J(t, K_1, K_2, T) \geq J^*(t, K_1, K_2, T)$. The welfare gain w for being able to diversify expressed as a fraction of capital is thus positive and follows from the indifference condition $J(t, K_1, K_2, T) = J^*(t, K_1(1+w), K_2(1+w), T)$, whose solution is

$$(11) \quad w = \left(\frac{J}{J^*}\right)^{\frac{1}{1-\gamma}} - 1.$$

We emphasize that the welfare gain from diversification depends on temperature and the share of brown capital, that is, $w = w(S, T)$, in a nonlinear manner (see Figure 4). The welfare gain w allows us to assess the effects of diversification under climate risk.

5. CALIBRATION

Table 1 summarizes our calibration with Appendix A.7 giving more details.

5.1. Economic Growth. In the past, the influence of climate change on asset markets was negligible and the historical impact of climate change on the economy was, if anything, modest, at least in developed countries (e.g., Dell et al., 2009, 2012). We therefore first calibrate production by disregarding climate damages. We then calibrate the damage specification.

Capital Shocks We set annual volatility of capital diffusion risk to $\sigma_1 = \sigma_2 = 0.02$ matching the observed volatility of consumption or output (e.g., Wachter 2013). We start with a benchmark value of $\rho_{12} = 0$ for the *instantaneous correlation* between the two capital stocks.¹⁵ Subsection E.7 in the online appendix discusses the influence of this correlation and presents the

¹⁵ This is also assumed by Cochrane et al. (2007) for an endowment economy.

TABLE 1
BENCHMARK CALIBRATION WITH 2020 AS BASE YEAR

Preferences		
δ	Time-preference rate (annual)	0.015
γ	Coefficient of relative risk aversion	4.355
ψ	Elasticity of intertemporal substitution	0.618
Economic Model		
Y_0	Initial GDP (trillion US \$, PPP)	103.55
S_0	Initial share of brown capital	0.94
A_1	Green total factor productivity	0.1058
A_2	Brown total factor productivity	0.1030
b_1	Green energy cost parameter	4.459×10^6
b_2	Fossil fuel cost parameter	2.307×10^6
ε_n	Price elasticity of energy supply	1.6
η_n	Energy share in production	0.066
ϕ_n	Investment adjustment cost parameter	39.08
φ	Dividend leverage parameter	2.8
σ_n	Annual capital volatility	0.02
α_e	Macroeconomic jump size parameter	8
λ_e	Macroeconomic disaster intensity parameter	0.088
κ	Capital reallocation cost parameter	2
ρ_{12}	Instantaneous correlation coefficient	0
Climate Model		
T_0	Initial temperature ($^{\circ}$ C)	1.27
σ_T	Temperature diffusion coefficient	0.015
ϑ	TCRE ($^{\circ}$ C/TtC)	1.8

effects for negative and positive ρ_{12} . Given the discussion in the previous section, the total correlation between the two capital stocks is significantly higher than indicated by the value of ρ_{12} .

We assume that the recovery rates, $Z_i = 1 - \ell_i$, $i \in \{e, c\}$, have power distributions over $(0,1)$ with parameters $\alpha_i > 0$, that is, the jump size distribution is determined by the density function $\zeta_i(Z_i) = \alpha_i Z_i^{\alpha_i-1}$, $Z_i \in (0, 1)$ (Pindyck and Wang 2013). The n th moment of the recovery rate is $\mathbb{E}[Z_i^n] = \frac{\alpha_i}{\alpha_i+n}$. We follow Barro and Jin (2011) and define a disaster as an event destroying more than $\bar{\ell}_e = 10\%$ of GDP or aggregate consumption. Their historical consumption data suggest an annual disaster probability of 3.8% and average consumption loss of 20% when a disaster occurs, so that $\mathbb{E}[\ell_e | \ell_e > \bar{\ell}_e] = 0.2$ and $\lambda_e \int_0^{1-\bar{\ell}_e} \zeta_e(Z_e) dZ_e = 0.038$. These conditions yield $\alpha_e = 8$ and $\lambda_e = 0.088$.

Dividends Empirically, dividends are more volatile than consumption and fall more than consumption when a disaster hits the economy (e.g., Bansal and Yaron, 2004; Wachter, 2013). This is because dividends are only a small contribution to household income, which is used to finance consumer spending. The largest part of household income is labor income, which is much less volatile than dividends. Following this literature, we model dividends in each sector as leveraged consumption, that is, $D_n = C_n^{\varphi}$, where we set the leverage parameter to $\varphi = 2.8$ leading to asset return volatilities much higher than consumption growth volatility. We follow this reduced-form approach because there is only one agent in our model. A more rigorous approach, in which capital is owned by intermediaries who issue stocks and pay dividends to households is beyond the scope of this article.¹⁶

¹⁶ In Subsection E.2 of the online appendix, we discuss alternative calibrations with unleveraged dividends, $D_n = C_n$ (cf. Cochrane et al., 2007; Pindyck and Wang, 2013; van den Bremer and van der Ploeg, 2021). Here, we also show that our results on diversification and asset pricing are robust to this assumption albeit optimal carbon prices are lower.

Production and Energy Costs Ignoring climate change, there is no price on carbon and optimal energy use gives a linear “AK” production function $Y_n = A_n^* K_n$ with productivity

$$(12) \quad A_n^* = A_n \frac{1+1/\varepsilon_n}{1-\eta_n+1/\varepsilon_n} \left(\frac{\eta_n}{b_n} \right)^{\frac{\eta_n}{1-\eta_n+1/\varepsilon_n}}.$$

To calibrate the EIS, risk aversion, adjustment costs, and total factor productivity, we use a special case of our model with an aggregate capital stock. Following Pindyck and Wang (2013), we choose these parameters to match a real expected growth rate of consumption of 2%, an average consumption fraction of GDP of $C/Y = 75\%$, an initial risk-free interest rate of $r_0^f = 0.8\%$ per annum, an average equity premium of 6.6% per annum, and a Tobin’s Q of $q = 1.548$. Given our choice of a relatively low time-preference rate of $\delta = 0.015$ (cf. Nordhaus, 2017), we use these data to back out a relative risk aversion of $\gamma = 4.355$, an EIS of $\psi = 0.618$, adjustment cost parameters of $\phi_1 = \phi_2 = 39.08$, and total factor productivities in (12) of $A_1^* = A_2^* = 0.0449$.¹⁷

Following van den Bremer and van der Ploeg (2021), we set the energy shares to be $\eta_n = 0.066$ and use an average global cost of fossil fuel of 540 USD per ton of carbon. We use a significantly higher average global price of green energy, that is, 810 USD for the same amount of energy,¹⁸ which is in line with production costs in developed countries such as Germany. Using a price elasticity of energy supply of $\varepsilon_n = 1.6$ (e.g., Png, 1999, p. 110), we determine cost parameters of $b_1 = 4.459 \cdot 10^6$ and $b_2 = 2.307 \cdot 10^6$ reflecting that green energy is significantly more expensive than fossil fuel.¹⁹ Solving (12) for A_n yields $A_1 = 0.1058$ and $A_2 = 0.1030$.

5.2. Damages from Global Warming. We consider two different climate damage specifications.²⁰ Our benchmark specification is the level impact from Nordhaus (2017), who uses $\Lambda_n(T) = 1 - \theta_n T^2$ and calibrates this so that damages at 3°C are 2.08% of predamages output. This gives a value of $\theta_n = 0.00236$.²¹

Complementary to our benchmark specification, we consider a model that is affected by climate disasters. Karydas and Xepapadeas (2022) collect data on climate-related events for 42 countries over the period from 1911 to 2015.²² Following the methodology of Loayza et al. (2012), they estimate climate-related disaster probabilities and magnitudes. Their model involves time-varying temperature disaster risk where the disaster intensity follows a mean-reversion process whose long-term mean is linear in temperature, $\bar{\lambda}_c(T) = \bar{\lambda}_{c0} + \bar{\lambda}_{c1} T$. Abstracting from mean reversion, we set $\lambda_c(T) = \lambda_{c0} + \lambda_{c1} T$ with $\lambda_{c0} = 0.003$ and $\lambda_{c1} = 0.096$. The process $\lambda_c(T)$ is approximately the probability that a disaster hits within the period of a year. Karydas and Xepapadeas (2022) report $\mathbb{E}[\ell_c] = 1.5\%$ for climate-related disasters. Using a power distribution for the recovery rate Z_c yields $\alpha_c = 65.67$. Figure A.1 in Appendix A.7 illustrates the calibration of climate disasters.

¹⁷ Alternatively, one could choose a higher value for the time-preference rate. Then, to match the risk-free rate of $r_0^f = 0.8\%$, a higher value of the EIS is needed. For instance, a calibration with $\delta = 0.0247$ and $\psi = 1.5$ yields almost identical results (available upon request). Since we have no information about whether the adjustment cost and total factor productivity parameters differ for the two sectors, we assume $\phi_1 = \phi_2$ and $A_1^* = A_2^*$ in our benchmark calibration. In Subsection E.10 of the online appendix, we consider an alternative calibration where these values differ for the two sectors.

¹⁸ We express energy in equivalent units of carbon emitted into the atmosphere.

¹⁹ Alternative calibrations for the cost parameters and the price elasticity of supply do not significantly affect our results (available upon request).

²⁰ See Subsection E.11 of the online appendix for a model involving both types of damages.

²¹ Nordhaus (2017) states that the damage function is inverse quadratic, $\Lambda_n(T) = \frac{1}{1+\theta_n T^2}$, whereas the corresponding GAMS code (General Algebraic Modeling Language) uses a quadratic damage function $\Lambda_n(T) = 1 - \theta_n T^2$. We have solved the model for both quadratic and inverse quadratic damage functions and the results are very similar.

²² They use the international disasters database EM-DAT, which is available at <https://www.emdat.be/>.

5.3. *Emission Intensity and Temperature Responses.* We calibrate the emission intensity ν per unit of fossil fuel such that under BAU, we match the RCP8.5 scenario of IPCC (2014). Historically, the emissions ratio has declined at a rate of 1.7% to 2% per year, a little less than the rate of economic growth. We model an emission intensity that steadily declines in expectation following:²³

$$dv_t = \nu_t \left[g_\nu dt - \frac{dY_t}{Y_t} \right],$$

where $g_\nu < \mathbb{E}[\frac{dY_t}{Y_t}]$ is a parameter determining the speed at which carbon emissions increase under BAU. Hence, carbon-dioxide emissions are given by $\epsilon_t = F_{2t}\nu_t$. This calibration ensures that carbon emissions are zero if the production of brown goods is zero.

Recent studies estimate a TCRE of 0.8 to 2.4° C/TtC (e.g., Allen et al., 2009; Matthews et al., 2009, 2018). We use a midrange value for the TCRE of $\beta = 1.8^\circ$ C/TtC. We set the reallocation cost parameter to $\kappa = 2$ so that the model predicts a temperature increase for 2100 of 1.8° C for the disaster impact. This calibration is in line with pledges made at the COP26 U.N. climate conference (IEA, 2021).²⁴

6. OPTIMAL CLIMATE POLICIES: TO ABATE OR DIVERSIFY?

To understand the economic effects of our optimal carbon price paths, we discuss two opposing effects. First, brown capital causes a negative externality that diminishes output, so the social planner seeks to cut the share of brown capital and thus emissions. This is the *abatement motive*. Second, the social planner is risk averse, so seeks to reduce total capital volatility which is driven by the share of brown capital. This is the *diversification motive*. We have done our best to have a calibration that fits the data and is as reasonable as our model permits, but we admit that our quantitative results primarily illustrate our model and insights, and must not be taken too literally. So, we offer a broad range of robustness checks in Section E of the online appendix to highlight the drivers of our results.

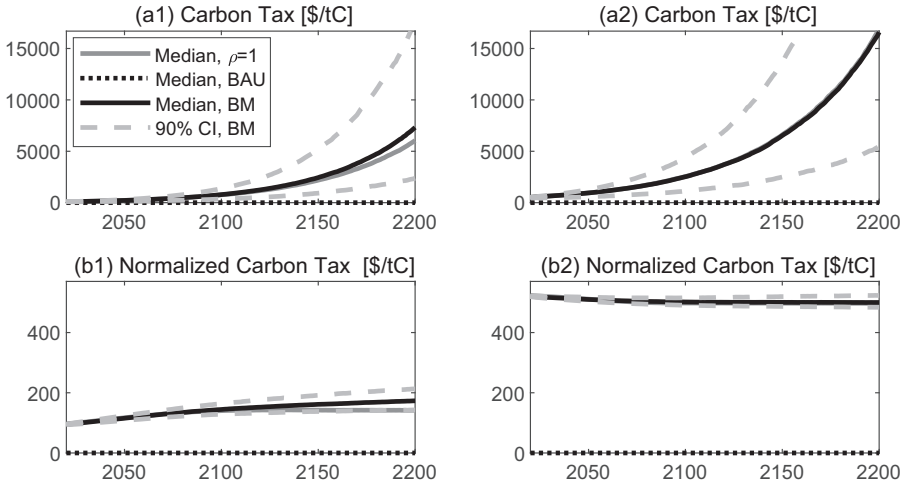
6.1. *Optimal Carbon Prices.* Panels (a1) and (a2) of Figure 1 show the median optimal carbon prices (—) and their 5% and 95% quantiles for the two damage specifications. The optimal median carbon tax starts in 2020 at 94 USD per ton of carbon (26 USD per ton of CO₂) for the level impact and at 505 USD per ton of carbon (138 USD per ton of CO₂) for the disaster impact. Since the optimal carbon tax is proportional to the aggregate stock of capital and GDP is proportional to the aggregate capital stock, the optimal carbon tax grows in line with the growth of the economy. Panels (b1) and (b2) of Figure 1 depict the carbon tax normalized by GDP (i.e., we multiply the carbon tax by initial GDP and divide by current GDP). This confirms that normalized carbon prices are roughly constant over time. If damages are sufficiently convex in temperature, the graph for normalized carbon prices will rise mildly as temperature increase.

Figure 1 also shows that median optimal carbon prices grow a bit slower if there are no benefits from diversification (—). This effect is not negligible, but carbon prices are primarily determined by the abatement motive and depend only to a limited extent on the diversification motive. Especially with climate disasters, the diversification effect is largely dominated by the abatement motive and carbon prices in both scenarios are almost identical.

Figure 2 shows how optimal carbon prices in the year 2020 depend on the share of brown capital S for the two damage specifications at a temperature anomaly of 1° C. This figure confirms our findings from Figure 1 but also highlights a state-dependent conflict between

²³ This requires no extra state variable as shocks to ν are perfectly correlated with those to Y .

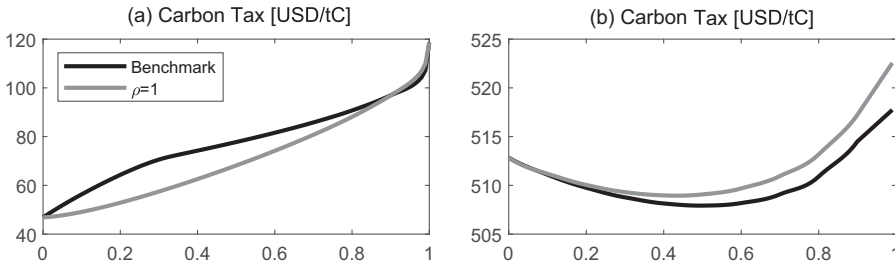
²⁴ Since this calibration is rather indirect, κ determines the speed of the transition toward a low-carbon economy and the stickiness of investment decisions, and there is very few data on this parameter available, we perform a sensitivity analysis in Subsection E.9 in the online appendix.



NOTES: The time paths of the optimal carbon prices for the two damage specifications level impact (first column) and disaster impact (second column) are depicted. The second row depicts carbon prices normalized for growth of the economy, that is, $\tau_c \frac{Y_0}{Y_t}$. Median optimal paths are depicted by black solid lines (—) and median BAU paths by dotted lines (⋯⋯). Dashed lines (---) show 5% and 95% quantiles of the optimal time paths. Gray lines (—) show the median optimal paths for a model without benefits from diversification because both capital stocks are perfectly correlated.

FIGURE 1

TIME PATHS FOR THE OPTIMAL CARBON TAXES FOR LEVEL AND DISASTER IMPACTS OF CLIMATE CHANGE



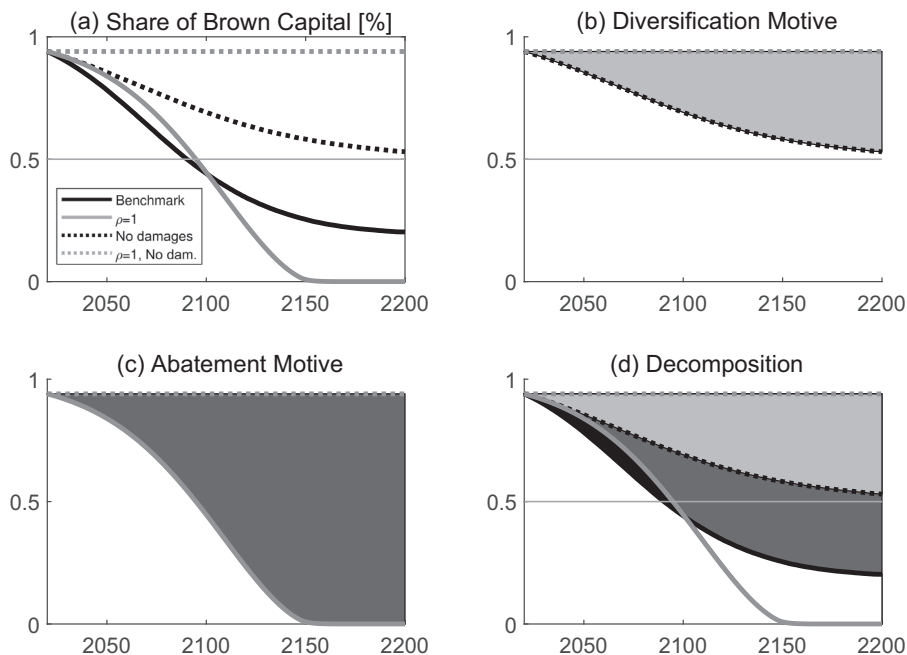
NOTES: The figure shows how optimal carbon prices in the year 2020 depend on the share of brown capital S for the two damage specifications level (TFP) impact (first column) and disaster impact (second column) at a temperature anomaly of 1°C . The black lines (—) depict the optimal carbon price in the benchmark specification. The gray lines (—) show the optimal prices in a model without benefits from diversification because both capital stocks are perfectly correlated. Similar figures for other years and different temperature anomalies are available upon request.

FIGURE 2

OPTIMAL CARBON TAXES AND SHARE OF BROWN CAPITAL FOR LEVEL AND DISASTER IMPACTS OF CLIMATE CHANGE

diversification needs and climate policy. This conflict is particularly pronounced for the level impact where the diversification motive plays no negligible role and the optimal carbon tax is heavily state-dependent. On the other hand, for a disaster impact the diversification motive is completely dominated by the abatement motive and the SCC is almost independent of S . We now discuss the abatement and diversification motives in greater detail.

6.2. *Results on Abatement and Diversification.* To decompose climate action into the parts that come from both motives, we consider four different calibrations to identify a pure diversification component, a pure abatement component, and an interaction term. Figure 3(a) plots the median optimal evolution of the share of brown capital for: (i) a model without damages from climate change and perfectly correlated diffusive risk, see gray dotted lines (---); (ii)



NOTES: The lines depict the optimal evolution of the share of brown capital until the year 2200 for (i) a model without damages from climate change and perfectly correlated diffusive risk, see gray dotted lines (---); (ii) a model without damages from climate change and zero instantaneous correlation, see black dotted lines (.....); (iii) a model with the Nordhaus damage specification and perfectly correlated diffusive risk, see gray lines (—); (iv) the benchmark model with the Nordhaus damage specification and zero correlation, see black solid lines (—). The areas in (b), (c), and (d) depict the strengths of the diversification motive (■), the strength of the abatement motive (■), and the interaction of diversification and abatement motives (■), in scenarios (ii), (iii), and (iv), respectively.

FIGURE 3

ABATEMENT AND DIVERSIFICATION MOTIVES WITH NORDHAUS LEVEL DAMAGES FROM CLIMATE CHANGE

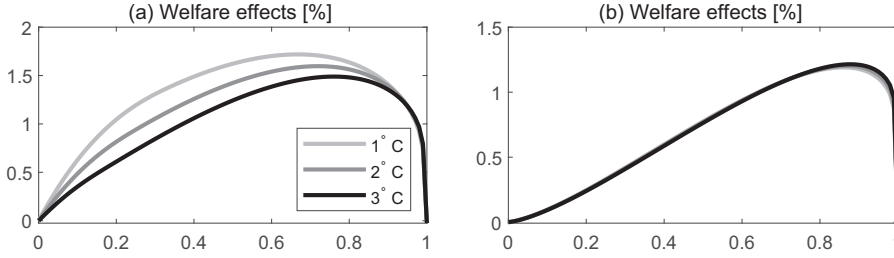
a model without damages from climate change and zero instantaneous correlation, see black dotted lines (.....); (iii) a model with the Nordhaus damage specification and perfectly correlated diffusive risk, see gray lines (—); (iv) our benchmark model with the Nordhaus damage specification and zero correlation,²⁵ see black solid lines (—).

For case (i), there is neither a diversification benefit nor any damage from climate change. The planner thus has no incentive to convert brown capital into green capital. For case (ii), the instantaneous correlation between the two capital stocks is zero and thus diversification is advantageous. Hence, the agent aims to achieve a diversified position which due to our calibration is reached at 50% brown capital.²⁶ Since in this calibration there are no damages from climate change, the transition is solely driven by the diversification motive. The light gray area (■) in Panel (b) depicts the diversification effect. For case (iii), capital stocks are perfectly correlated capital stocks, so that there is no diversification benefit. Consequently, the transition toward a zero-carbon economy in Panel (c) is solely driven by the abatement motive, which is represented by the dark gray area (■).

Finally, we study the benchmark (iv) with zero correlation and Nordhaus damages depicted in Panel (d). It turns out that the share of brown capital optimally stabilizes in between the two polar cases (ii) and (iii). This shows that there is an interaction effect. Initially, the

²⁵ The total correlation between the two capital stocks and, in turn, between asset prices is significantly driven by macroeconomic disasters. Since both capital stocks suffer common macroeconomic shocks via N^e , the total correlation between the capital stocks is significantly higher than the instantaneous diffusive correlation ρ_{12} . Our numerical simulations indicate that the total correlation coefficient is always higher than 90%.

²⁶ If there are N energy sectors, none correlated, the optimal allocation between these sectors is $1/N$.



NOTES: Panel (a) plots the welfare gain from diversification (11) as function of the share of brown capital S for a Nordhaus level impact (evaluated at three temperatures) and Panel (b) for a rare disasters impact.

FIGURE 4

WELFARE GAINS FROM DIVERSIFICATION VERSUS SHARE OF BROWN CAPITAL, S

diversification motive fosters the transition toward a low-carbon economy. Compared to the case with perfect correlation, the transition takes place at a faster rate, leading to more abatement in response to diversification effects. This is visualized by the black area (■) in Panel (d). In the long run, however, the two goals become conflicting and a trade-off arises. This happens around the year 2100 when the capital stocks are fully diversified. From this point onward, the diversification motive hampers the transition, which eventually stabilizes at about 20% of brown capital. It is thus beneficial to keep some carbon-intensive capital in the economy to reap the benefits of diversification. We have thus decomposed climate action into three components:

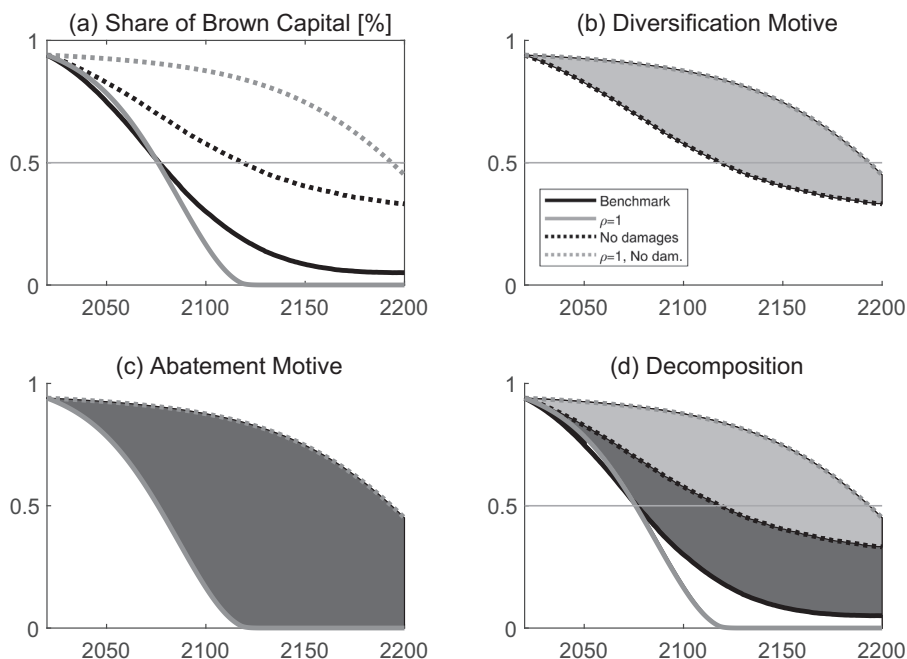
$$\text{Climate Action} = \text{Diversification (■)} + \text{Abatement (■)} + \text{Interaction (■)}.$$

The decomposition shown in Figure 3 can be carried out for other type of damages and correlation structures too. For instance, for the disaster impact, the damages are significantly more pronounced than for the level impact, and the abatement motive dominates the diversification motive. Hence, the carbon-intensive capital stock is eventually run down completely, so that the dark gray area becomes bigger (see Figure A.7 in the online appendix). Furthermore, a higher (lower) instantaneous correlation ρ_{12} reduces (increases) the benefit of diversification and thus lowers (increases) the level at which the share of brown capital stabilizes in the long run (see Subsection E.7 in the online appendix).²⁷ The brown capital stock is then eventually eliminated and no more CO_2 is emitted. However, if diversification effects prevail and the company keeps part of the brown capital stock in operation, a higher carbon price is needed to control emissions.

Figure 4 plots the welfare gains of diversification under climate risk computed from Equation (11). We see that the benefits from diversification can reach more than 1.5% of global output depending on the share of brown capital and temperature. This benefit can exceed the damages from global warming under the DICE damage specification. The figure also illustrates that the welfare gains are larger if temperatures are smaller, which stems from damages being a convex function of temperature. In case of climate disasters, the negative impact of keeping the share of brown capital in operation can easily exceed the benefits from diversification and the welfare effects are less sensitive to current temperatures.

6.3. Extension: LBD in Green Production. So far, we have assumed that there is no directed technological change (e.g., Acemoglu et al., 2012; Casey, 2024). Here, we address the question of how technological change affects the transition toward a low-carbon economy in the presence of diversification motives. For this purpose, we allow the costs of renewable energy to decrease endogenously along the transition path driven by LBD in the production of green goods. This leads to path-dependent energy prices and a more efficient green sector in

²⁷ Subsection E.7 also delivers an explanation why median optimal carbon prices are a bit lower in the long run if there are no or only dominated benefits from diversification (see Subsection 6.1).



NOTES: The lines depict the optimal evolution of the share of brown capital until the year 2200 for (i) a model without climate damages and perfectly correlated diffusive risk, see gray dotted lines (---); (ii) a model without climate damages and zero instantaneous correlation, see black dotted lines (.....); (iii) a model with the Nordhaus damage specification and perfectly correlated diffusive risk, see gray lines (—); and (iv) the benchmark model with the Nordhaus damage specification and uncorrelated diffusive risk. The areas in (b), (c), and (d) depict the strengths of the diversification motive (■), the strength of the abatement motive (■), and the interaction of diversification and abatement motives (■), in scenarios (ii), (iii), and (iv), respectively.

FIGURE 5

ABATEMENT AND DIVERSIFICATION MOTIVES WITH ACCELERATED GREEN TRANSITION DRIVEN BY DIRECTED TECHNOLOGICAL CHANGE

the long run. This gives an additional incentive to restructure the economy away from fossil fuel toward green energy, even if diversification and abatement motives do not play a role. We call this new motive the *LBD motive*, which is a different form of directed technical change that occurs in upcoming green instead of in mature brown industries (and is a complementary approach to reallocating scientists from the brown to the green sector).

Figure 5 studies the interaction between the abatement motive, the diversification motive, and the LBD motive in a model with a degree of path dependency. For this purpose, we assume that the cost parameter for green energy gradually converges to that for fossil fuels as the green transition progresses. More specifically, $b_1(S) = k_0(1 - S)^{-k_1}$, where the parameters k_0 and k_1 are calibrated such that energy costs before carbon taxes for both sectors are identical when the transition has been completed and that initially the costs for renewable energy correspond to the costs as in the benchmark calibration.²⁸

Compared to our benchmark model, the share of brown capital now decreases over time even in a model without benefits from diversification or abatement. This decrease as shown in (---) is thus due to the LBD motive stemming from path-dependent energy efficiency. Figure 5 illustrates that the main results obtained from Figure 3 are still valid. Initially, the

²⁸ Formally, this requires $b_1(S_0 = 0.94) = b_1 = 4.459 \cdot 10^6$ and $b_1(0) = b_2$, that is, $(1 - S_0)^{-k_1} = 1$ or $k_1 = 0.2342$ and $k_0 = b_2 = 2.307 \cdot 10^6$. An alternative calibration based on the historical price development of solar modules corresponds to a cost reduction of green goods of about 20% for every doubling of solar panels in use (de la Tour et al., 2013). This leads to a more pronounced path dependency (see Subsection E.4 in the online appendix). Our main results carry over but the diversification motive becomes less relevant although it still is economically significant.

diversification motive accelerates the transition toward a low-carbon economy. In the long run, however, the two goals become conflicting and a trade-off arises.

Finally, Figure A.9 in the online appendix shows the optimal carbon price and compares it to the one in the benchmark specification without LBD. We see that with LBD the optimal carbon price is a bit lower as the transition toward a low-carbon economy is slightly accelerated by the LBD motive. This is well in line with Panel (c) of Figure 5, where the abatement motive is less pronounced than in the benchmark case.

7. ASSET PRICING IMPLICATIONS

This section discusses the implications of climate policy on asset prices for the benchmark model. Results carry over to the LBD extension available upon request.

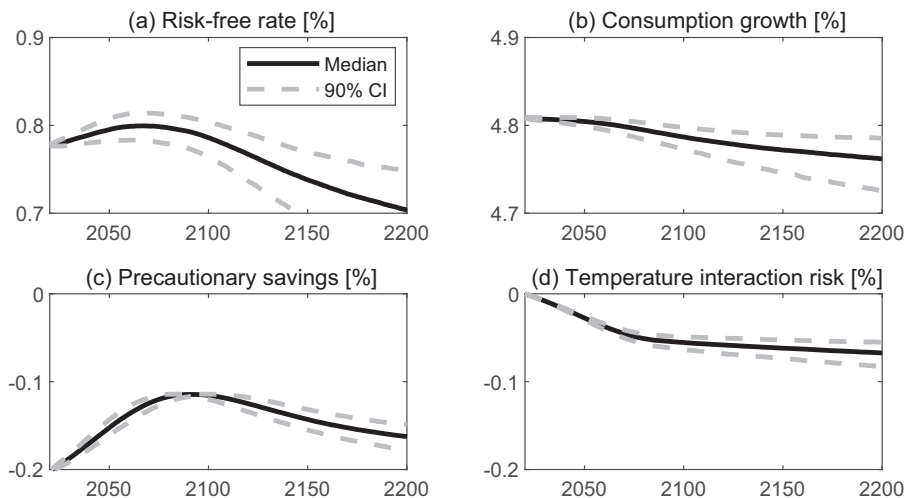
7.1. Risk-Free Rate and Precautionary Savings. Here, we show how the share of brown capital and temperature affect precautionary savings and the risk-free rate. In equilibrium, the risk-free rate r^f (see Appendix A.3) is given by

$$(13) \quad r_t^f = \delta + \frac{1}{\psi} \mu_C - \underbrace{\frac{1}{2} \gamma \left(1 + \frac{1}{\psi}\right) \|\sigma_C\|^2}_{\text{diffusion risk}} - \underbrace{\sum_{i \in \{e, c\}} \lambda_i(T) \mathbb{E} \left[1 - (1 - \ell_i)^{-\gamma} + \frac{\psi^{-1} - \gamma}{1 - \gamma} (1 - (1 - \ell_i)^{1-\gamma}) \right]}_{\text{risk of rare disasters}} \\ + \underbrace{\frac{\gamma \psi - 1}{2\psi^2} (\|\sigma_C - \sigma_k\|^2 + \psi (\|\sigma_C\|^2 - \|\sigma_k\|^2)) + \frac{\theta - 1}{\psi \theta} \sigma_g^\top (\sigma_C - \sigma_k)}_{\text{temperature interaction risk}}.$$

Equation (13) offers a similar decomposition of the risk-free interest rate (cf. Barro, 2006, 2009; Pindyck and Wang, 2013; Wachter, 2013). The first two terms in Equation (13) also arise in deterministic models: if the time-preference rate δ is high, there are strong preferences for early consumption and one would thus like to borrow. Since, in equilibrium, the risk-free asset is in zero net supply, the risk-free rate must increase to counter this. Besides, the risk-free rate increases in the expected growth rate of consumption μ_C due to the agent's attitude toward smooth consumption streams, which is driven by the EIS ψ . Table A.1 in Online Appendix C shows that the expected consumption growth rate μ_C falls with temperature, but is almost independent of S . The negative effect of temperature reflects the impact of climate change on output echoed in other IAMs.

The third term $-\frac{1}{2} \gamma (1 + \frac{1}{\psi}) \|\sigma_C\|^2$ in Equation (13) represents the motive for precautionary savings in response to diffusion risk, which requires the interest rate to fall to keep the risk-free asset in zero net supply. The expected consumption growth rate and its volatility depend nonlinearly on both the temperature and the brown capital share, whereby the result is more involved and qualitatively different from one-tree endowment economies. Although the effect of temperature on the precautionary-savings term $-\frac{1}{2} \gamma (1 + \frac{1}{\psi}) \|\sigma_C\|^2$ is negligible, Table A.1 indicates that the share of brown capital has a significant influence on the equilibrium risk-free rate. The latter result stems from a diversification argument (cf. Cochrane et al., 2007). Diversifying across the green and brown capital stocks reduces the volatility of the total capital stock and this effect carries over to aggregate consumption. If climate policy drives the share of brown capital below S^* in (10), the consumption stream becomes riskier again and the demand for precautionary savings increases. This explains the nonmonotonic behavior of the consumption volatility and, in turn, the nonmonotonic relation between the share of brown capital and the equilibrium risk-free rate.

The fourth term $-\sum_{i \in \{e, c\}} \lambda_i(T) \mathbb{E} [1 - (1 - \ell_i)^{-\gamma} + \frac{\psi^{-1} - \gamma}{1 - \gamma} (1 - (1 - \ell_i)^{1-\gamma})]$ in Equation (13) reflects precautionary savings in response to rare disaster risks. As for standard diffusion risk, these terms reduce the interest rate to keep the risk-free asset in zero net supply. The



NOTES: Panel (a) depicts the time paths for the risk-free rate with level damages whereas Panels (b), (c) and (d) plot the state-dependent components related to consumption growth $\frac{1}{\psi}\mu_C$, precautionary savings from diffusion risk $-\frac{1}{2}\gamma(1 + \frac{1}{\psi})\|\sigma_C\|^2$, and temperature interaction terms, respectively. Median optimal paths are depicted by solid lines (—) and dashed lines (---) show 5% and 95% quantiles of the optimal time paths.

FIGURE 6

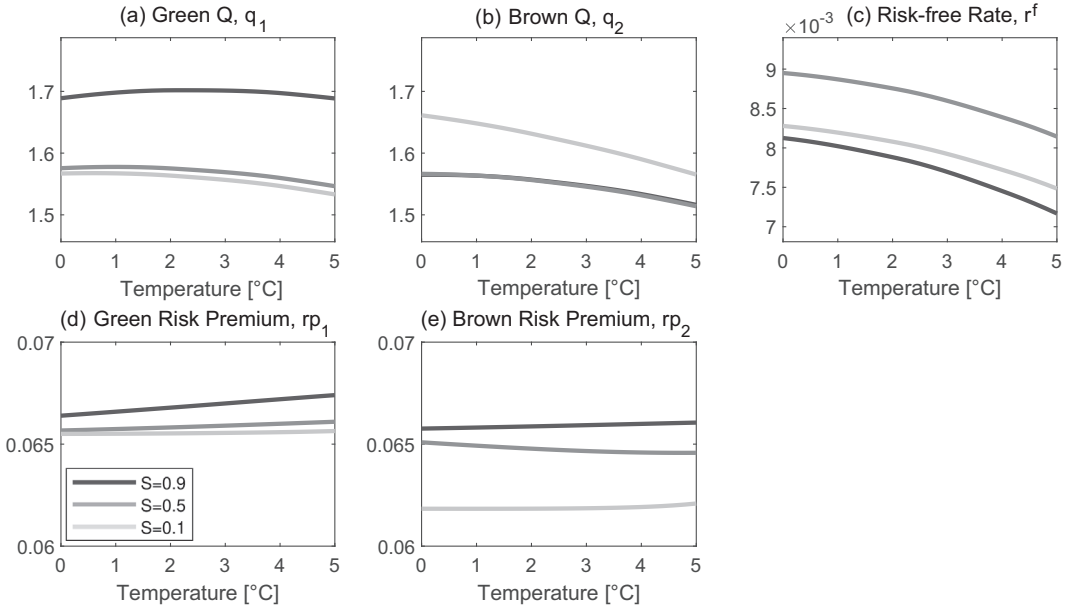
TIME PATHS OF THE EQUILIBRIUM RISK-FREE RATE

greater the risk aversion, the greater is this effect, see also the extensive discussion in Wachter (2013). A novel feature is that the jump intensity for climate disaster risk λ_c increases in temperature, so that higher temperatures curb the risk-free interest rate. Therefore, a less ambitious climate policy implies a strong increase in the demand for precautionary savings and lower interest rates in the long term.

The temperature interaction risk terms in the second row in Equation (13) capture the interdependence between capital, consumption, temperature, and the value function. Compared to Cochrane et al. (2007), these terms are novel and result from the inability to hedge temperature shocks. They represent precautionary savings for uninsurable temperature risk. We emphasize that these components depend on the relevant state variables, in particular on temperature, in a nonlinear manner, but they have little influence on the risk-free rate because consumption volatility σ_C is close to capital volatility. In case of time-additive CRRA utility ($\gamma = 1/\psi$ or equivalently, $\theta = 1$), these terms add up to zero.

Figure 6(a) shows the evolution of the equilibrium risk-free rate over time for the level impact of damages. Median optimal paths are depicted by solid lines (—). Dashed lines (---) show 5% and 95% quantiles of the optimal time paths. Since temperatures tend to increase over time and the effect of higher temperatures on consumption growth is negative, there is a slight downward trend in $\frac{1}{\psi}\mu_C$ in Panel (b). Panel (c) shows the simulation of the precautionary savings component in response to diffusion risk, which reacts to the share of brown capital in a nonlinear manner. This component is smallest in absolute terms when the economy is perfectly diversified slightly before the year 2100. From this point onward, the demand for precautionary savings increases again since the transition toward a poorly diversified low-carbon economy is still ongoing. Panel (d) depicts the precautionary savings component for temperature interaction risk. It is not surprising that this demand increases in response to higher temperatures. Overall, the effect of those components is relatively small compared to the disaster risk component in Equation (13).²⁹

²⁹ Similar decompositions for other scenarios and damage specifications are available upon request.



NOTES: The lines represent various levels of the capital share: dark lines (—) depict $S = 0.9$, gray lines (—) refer to $S = 0.5$, and light (—) lines to $S = 0.1$. Panel (a) plots Tobin's Q of the green asset, (b) shows Tobin's Q of the brown capital stock, (c) depicts the equilibrium risk-free rate, (d) shows the risk premium of the green asset, and (e) depicts the risk premium of the brown asset. The option to convert brown capital into green capital generates interesting qualitative effects but the quantitative implications are moderate.

FIGURE 7

ASSET PRICES VERSUS TEMPERATURE AND THE SHARE OF BROWN CAPITAL (NORDHAUS LEVEL DAMAGES FROM CLIMATE CHANGE)

7.2. Risk Premia and Tobin's Q.

Results for the Level Damage Calibration by Nordhaus Panels (a) and (b) of Figure 7 show that the Tobin's Q for both the green and the brown sector falls with temperature. The opposite is true for the book-to-market ratio. This implies that for a fixed amount of capital the market value decreases in temperature, both for the green and brown asset. Panel (a) shows that the Tobin's Q of the green asset increases in the share of brown capital. Therefore, for a fixed amount of capital the green asset has a higher market value if the economy is more carbon-intensive. Panel (b) indicates that the opposite is true for the carbon-emitting asset. Panel (c) shows the equilibrium risk-free rate, whose behavior has already been discussed above.

Panels (d) and (e) show how the brown and the green risk premia vary with temperature for given shares of brown capital. Notice that the economy has the option to convert brown into green capital at some adjustment costs. To better understand the patterns, we consider Figure A.2 in the online appendix, which is analogous to Figure 7, but disregards the option to convert. First, it can be seen in Panels (d) and (e) that the risk premia of the brown and green sectors are positively related to their shares, S and $1 - S$, respectively, which is qualitatively similar to Cochrane et al. (2007). Second, there is hardly any temperature dependence, which indicates that the variation in the shares of capital in Figure A.2 is mainly driven by the diversification motive. The asset which is scarce thus carries the highest risk premium.

If the option to convert brown capital is now taken into account, the value of the brown asset involves the value of this option. For situations with high shares of brown capital and currently low temperatures, the option is relatively more valuable. This can be seen in Figure 7. In turn, the green asset is relatively less valuable and the green premium is higher as long as the brown capital share is large. Eventually, when the brown capital share is small the brown

TABLE 2
CARBON RISK PREMIUM

	Level Impact						Climate Disasters					
	Optimal			Business as Usual			Optimal			Business as Usual		
	rp_1	rp_2	$rp_2 - rp_1$	rp_1	rp_2	$rp_2 - rp_1$	rp_1	rp_2	$rp_2 - rp_1$	rp_1	rp_2	$rp_2 - rp_1$
$T = 1^\circ \text{C}$	6.58%	6.48%	-0.11%	6.16%	6.56%	0.40%	6.67%	6.77%	0.10%	6.24%	6.63%	0.39%
$T = 2^\circ \text{C}$	6.60%	6.45%	-0.14%	6.17%	6.57%	0.40%	6.74%	6.83%	0.09%	6.32%	6.71%	0.39%
$T = 3^\circ \text{C}$	6.61%	6.44%	-0.16%	6.17%	6.57%	0.40%	6.82%	6.89%	0.08%	6.40%	6.79%	0.39%
$T = 4^\circ \text{C}$	6.62%	6.45%	-0.17%	6.17%	6.57%	0.40%	6.89%	6.96%	0.07%	6.48%	6.86%	0.38%
$T = 5^\circ \text{C}$	6.63%	6.46%	-0.17%	6.18%	6.58%	0.40%	6.96%	7.02%	0.06%	6.55%	6.94%	0.38%
$S = 0.10$	6.56%	6.20%	-0.35%	6.57%	6.19%	-0.38%	6.72%	6.70%	-0.02%	6.90%	6.51%	-0.39%
$S = 0.25$	6.61%	6.27%	-0.34%	6.50%	6.27%	-0.24%	6.72%	6.61%	-0.10%	6.84%	6.56%	-0.28%
$S = 0.50$	6.61%	6.44%	-0.17%	6.40%	6.38%	-0.03%	6.74%	6.64%	-0.10%	6.73%	6.67%	-0.06%
$S = 0.75$	6.66%	6.53%	-0.13%	6.29%	6.49%	0.20%	6.80%	6.72%	-0.08%	6.62%	6.80%	0.18%
$S = 0.90$	6.73%	6.61%	-0.12%	6.20%	6.56%	0.36%	6.84%	6.75%	-0.08%	6.53%	6.88%	0.35%

NOTE: The table shows the risk premia for the two assets and the carbon premium, defined as the difference between the risk premia of the two assets, for the optimal run and BAU scenarios. It provides sensitivity analysis for different values of the share of brown capital and temperature around their median values in 2100 ($S = 0.44$, $T = 2.9^\circ \text{C}$ for the optimal run and $S = 0.93$, $T = 4.4^\circ \text{C}$ for BAU). Based on the benchmark calibration (see Section 5).

premium is about the same with and without the option to convert, since the option has then lost its value. This becomes clear when comparing the light lines in Panel (e) of Figures 7 and A.2. The same is true for the green premium.

Table 2 reports the risk premia of the green and brown asset, rp_1 and rp_2 , in the optimal and in the BAU scenario. It can be seen that all values are between 6.17% and 6.73%. Furthermore, the table provides the differences between these risk premia which we refer to as the *carbon premium* (cf. Bolton and Kacperczyk, 2021). In line with this literature, we find a positive carbon premium of about 0.4% for the BAU scenario with $S = 0.9$. This carbon premium declines and becomes eventually negative if the brown capital stock decreases. In the optimal case, society prices carbon dioxide appropriately, and thus the carbon premium declines even more and can be negative. Notice that variation in temperature has a minor influence on the carbon premium. Therefore, an ambitious climate policy that reduces the share of brown capital turns the positive carbon premium into a negative one.

This is also in line with the recent findings of Bauer et al. (2022), Zhang (2024), and Aswani et al. (2024), which challenge the existence of carbon and pollution premiums as in Bolton and Kacperczyk (2021, 2023) and Hsu et al. (2023). In fact, our model can explain a positive carbon or pollution premium if carbon dioxide is not properly priced and the negative externality has not been internalized. However, if society starts pricing carbon emissions, our model can also explain higher expected rate of returns of green portfolios. Moreover, our model generates price paths for green firms' stock prices that tend to increase over time more rapidly than brown firms' prices, which is well in line with Pastor et al. (2021, 2022), who demonstrate that green firms generate higher realized returns than brown firms and their implied cost of capital is smaller than for their brown counterparts. Pastor et al. (2021) identify two ways green demands can shift. First, investors' demand for green assets can increase, directly driving up green asset prices. Second, consumers' demand for green products can increase, for example, due to environmental preferences, boosting green firms' profits and stock prices. Pastor et al. (2022) also predict that green firms tend to outperform brown firms when concerns about climate change increase. Ardia et al. (2023) tested this prediction empirically using data for S&P 500 companies from January 2010 to June 2018.

Results for the Damage Calibration with Climate Disasters Figure A.3 in the online appendix depicts the asset pricing implications for the disaster impact. Since the disaster intensity grows linearly in temperature, this linearity carries over to the relevant asset pricing quan-

tities. Most of the qualitative results obtained by the Nordhaus damage specification persist for the jump impact. The most important findings are that with climate disasters the equilibrium risk-free rate is *negatively* affected and the risk premia are *positively* affected by temperature. In contrast to the Nordhaus specification, economic damages involve tipping risks that increase with temperature and their magnitudes are modeled by a right-skewed power distribution. This yields another dimension of risk, for which investors want to be compensated. Furthermore, there is also a carbon risk premium in the BAU scenario as in the previous paragraph, which declines substantially as carbon is priced (see Table 2).

8. CONCLUSION

Our main concern has been the interplay between climate action and financial considerations. Since agents want to hold diversified asset holdings, the transition toward a low-carbon economy is affected by diversification motives. Diversification and climate action are initially complementary goals, since agents want to decarbonize the economy and hold a balanced portfolio of green (carbon-free) and brown (carbon-intensive) assets. At some point during the green transition, however, the two goals become conflicting and a trade-off arises. This is because environmental considerations incentivize the economy to further reduce the brown capital share, but in turn assets holdings become less diversified. Climate policy is thus frustrated by the need to diversify financial asset holdings. Furthermore, if damages from climate change are moderate as in the DICE model, it is not optimal to fully run down the brown sectors as they serve as a hedge in the long run. Keeping the brown sectors open in the short run allows a faster buildup of green assets. If the adverse impact of global warming on economic activity is much more pronounced than suggested by DICE, it is optimal to close down the brown sectors completely.

Our results suggest that policymakers should initially be intrinsically motivated to take climate action, simply to reach diversified asset holdings. Only if policymakers want to speed up the process, they must take extra action. Later in the process of the green transition, matters change fundamentally. If policymakers wish to incentivize the economy to reduce the brown capital stock beyond its fully diversified share, they must counter the effects of diversification. These insights regarding the changing importance of diversification and abatement during the green transition also hold if we allow the cost of green goods to fall as more experience is accumulated by producing these goods (cf. Swanson's and Wright's law), but the green transition will be accelerated.

We have shown that the risk-free rate falls as climatic and other shocks increase. This reflects the precautionary saving motive. Furthermore, we have shown that potential climate disasters are crucial for a significant effect of climate change on asset prices. We have also analyzed a situation where the economy is stuck in a BAU scenario and does not take climate action. We have shown that compared to the optimal solution, the equilibrium interest rates fall substantially and the carbon premium is higher and positive. This indicates that being stuck in the BAU scenario does not only hurt the real economy, but can also distort the allocation of capital in financial markets as interest rates and risk premia are biased.

As for further research, more empirical evidence is needed on how climate policy affects the return on and prices of financial assets, both in sectors that make substantial use of fossil fuel and others that make more use of renewable energy. In particular, evidence is needed on the covariance of macroeconomic shocks, both normal macroeconomic shocks and climate-related disaster shocks, hitting the brown and green sectors to assess how important the asset diversification and hedging arguments are during the green transition.

Furthermore, our model is well-suited to consider the impacts of uncertainties about future climate policies, breakthrough technologies, and sudden shifts to greener preferences on the stranding of financial assets, asset returns, carbon risk, and other risk premia.³⁰ Bolton

³⁰ A survey of stranded carbon-intensive assets is provided by van der Ploeg and Rezai (2020).

and Kacperczyk (2021, 2023) find that stocks of companies with higher emissions earn higher returns, even after controlling for size, book to market, momentum, and other factors that predict returns. These carbon risk premia have been rising and cannot be explained by unexpected profitability or other risk premia.³¹ They may be explained by transition risk (cf. Barnett, 2023b; Hsu et al., 2023), so in future work it is important to investigate this risk in a stochastic IAM.

DATA AVAILABILITY STATEMENT The codes and data that support the findings of this study are openly available in OPENICPSR at <http://doi.org/10.3886/E198001V1>, reference number: openicpsr-198001.

APPENDIX A

A.1. *Reduced-Form Value Function.* Following Duffie and Epstein (1992b), the value function $J = J(t, K_1, K_2, T)$ satisfies the Hamilton–Jacobi–Bellman (HJB) equation

$$\begin{aligned}
 0 &= \max_{I_1, I_2, R, F_1, F_2} \left\{ J_t + \delta \theta J \left[\frac{\left(\sum_{n=1,2} Y_n - I_n - \frac{b_n K_n^{-1/\varepsilon_n}}{1+1/\varepsilon_n} F_n^{1+1/\varepsilon_n} \right)^{1-1/\psi}}{[(1-\gamma)J]^{1/\theta}} - 1 \right] + J_T \beta F_2 \right. \\
 &\quad + \frac{1}{2} J_{TT} \sigma_T^2 + J_{K_1} \left(I_1 - \frac{1}{2} \phi_1 \frac{I_1^2}{K_1} + R - \frac{1}{2} \kappa \frac{R^2}{K_1} - \delta_1^k K_1 \right) + \frac{1}{2} J_{K_1 K_1} K_1^2 \sigma_1^2 \\
 (A.1) \quad &\quad + J_{K_2} \left(I_2 - \frac{1}{2} \phi_2 \frac{I_2^2}{K_2} - R - \delta_2^k K_2 \right) + \frac{1}{2} J_{K_2 K_2} K_2^2 \sigma_2^2 + J_{K_1 K_2} K_1 K_2 \sigma_1 \sigma_2 \rho_{12} \\
 &\quad \left. + \lambda_e \mathbb{E}[J(K_1(1 - \ell_e), K_2(1 - \ell_e), T) - J] + \lambda_c(T) \mathbb{E}[J(K_1(1 - \ell_c), K_2(1 - \ell_c), T) - J] \right\},
 \end{aligned}$$

where subscripts of J denote partial derivatives, for example, $J_{K_1} = \frac{\partial J}{\partial K_1}$. To solve the HJB equation (A.1), we first transform it by expressing decision variables in relative terms and reduce the number of state variables by one. Let $i_n = I_n/K_n$, $f_n = F_n/K_n$, $r = R/K_1$, and $c = C/K$ denote the relative control variables. We express the value function in terms of time, total capital $K = K_1 + K_2$, share of brown capital $S = K_2/(K_1 + K_2)$, and temperature T (instead of K_1, K_2 , and T). Defining $S_1 = 1 - S$, $S_2 = S$, the production functions become

$$Y_n = A_n S_n K f_n^{\eta_n} \Lambda_n(T).$$

The amounts of consumption goods produced by each sector are

$$C_n = S_n K \left[A_n f_n^{\eta_n} \Lambda_n(T) - i_n - \frac{b_n}{1+1/\varepsilon_n} f_n^{1+1/\varepsilon_n} \right].$$

Therefore, aggregate consumption satisfies

$$(A.2) \quad c = \sum_{n=1,2} S_n \left[A_n f_n^{\eta_n} \Lambda_n(T) - i_n - \frac{b_n}{1+1/\varepsilon_n} f_n^{1+1/\varepsilon_n} \right].$$

The dynamics of the state variables can be written as

$$\begin{aligned}
 dK_1 &= K_1 - \left[\left(i_1 - \frac{1}{2} \phi_1 i_1^2 + r - \frac{1}{2} \kappa r^2 - \delta_1^k \right) dt + \sigma_1 dW_1 - (\ell_e dN_e + \ell_c dN_c) \right], \\
 dK_2 &= K_2 - \left[\left(i_2 - \frac{1}{2} \phi_2 i_2^2 - r \frac{K_1}{K_2} - \delta_2^k \right) dt + \sigma_2 \left(\rho_{12} dW_1 + \sqrt{1 - \rho_{12}^2} dW_2 \right) - (\ell_e dN_e + \ell_c dN_c) \right],
 \end{aligned}$$

³¹ Donadelli et al. (2017) show that increasing awareness of the global warming challenge has led to increasing carbon risk premia. The evidence suggests that markets have started to price in the climate transition from 2015 onward. Hsu et al. (2023) provide evidence for pollution risk premia of about 4.4%/year and use data on environmental litigation penalties to suggest that these are linked to regime change risk.

$$dT = \widehat{\beta} f_2 dt + \sigma_T(T) dW_3,$$

where $\widehat{\beta} = \beta/K_2$. To shorten the notation, we write $W = (W_1, W_2, W_3)^\top$ and denote the drift of the capital stocks and temperature by μ_{K_i} and μ_T , respectively. Ito's lemma gives the dynamics of K and S :

$$\begin{aligned} dS &= S(1-S) \left[\mu_S(i_1, i_2, r, S) dt + (\sigma_2 \rho_{12} - \sigma_1) dW_1 + \sigma_2 \sqrt{1 - \rho_{12}^2} dW_2 \right], \\ dK &= K_- \left[\mu_K(i_1, i_2, r, S) dt + [(1-S)\sigma_1 + S\sigma_2 \rho_{12}] dW_1 + S\sigma_2 \sqrt{1 - \rho_{12}^2} dW_2 - (\ell_e dN_e + \ell_c dN_c) \right], \end{aligned}$$

where the drifts are given by³²

$$\begin{aligned} \mu_S(i_1, i_2, r, S) &= \mu_{K_2} - \mu_{K_1} + S(\sigma_1 \sigma_2 \rho_{12} - \sigma_2^2) + (1-S)(\sigma_1^2 - \sigma_1 \sigma_2 \rho_{12}), \\ \mu_K(i_1, i_2, r, S) &= (1-S)\mu_{K_1} + S\mu_{K_2}. \end{aligned}$$

We thus solve a modified HJB equation with finite differences in terms of only two (S, T) instead of three state variables (K_1, K_2, T) . The following proposition summarizes our findings.

PROPOSITION A.1 (VALUE FUNCTION AND OPTIMAL CONTROLS). *Suppose $\widehat{\beta} = \widehat{\beta}(t, S, T)$. The value function (4) has the form*

$$(A.3) \quad J(t, K_1, K_2, T) = \frac{1}{1-\gamma} (K_1 + K_2)^{1-\gamma} G(t, T, S(K_1, K_2)).$$

where G satisfies a certain HJB equation which is given in (A.10) below. The optimal reallocation strategy from brown to green capital is

$$(A.4) \quad r = \frac{1}{\kappa} \left(\frac{G_S}{G_S S + (\gamma-1)G} \right).$$

Optimal green energy use is

$$(A.5) \quad f_1 = \left(\frac{b_1}{\eta_1 A_1 \Lambda_1(T)} \right)^{\frac{1}{\eta_1 - 1 - \varepsilon_1}}.$$

The optimal investment strategies and fossil fuel use follow from the nonlinear equations:

$$(A.6) \quad \delta(1-\gamma)G^{1-1/\theta} c^{-1/\psi} = [(1-\gamma)G - G_S S][1 - \varphi_1 i_1],$$

$$(A.7) \quad \delta(1-\gamma)G^{1-1/\theta} c^{-1/\psi} = [(1-\gamma)G + G_S(1-S)][1 - \varphi_2 i_2],$$

$$(A.8) \quad \delta(1-\gamma)G^{1-1/\theta} c^{-1/\psi} = -\frac{G_T \beta}{A_2 \Lambda_2 \eta_2 f_2^{\eta_2 - 1} - b_2 f_2^{1/\varepsilon}}.$$

The optimal social cost of carbon is

$$(A.9) \quad \tau_c = \frac{\vartheta C^{1/\psi}}{\delta(\gamma-1)} \frac{G_T}{G^{1-1/\theta}},$$

where optimal consumption is (A.2).

PROOF. Let $i_n = I_n/K_n$, $f_n = F_n/K_n$, $r = R/K_1$ denote the control variables in relative terms. Substituting these relative controls into (A.1) leads to the HJB equation:

$$0 = \sup_{i_1, i_2, f_1, f_2, r} \left\{ \frac{\delta}{1-1/\psi} [(1-\gamma)J]^{1-1/\theta} \left(\sum_{n=1,2} S_n (K_1 + K_2) \left[A_n f_n^{\eta_n} \Lambda_n(T) - i_n - \frac{b_n}{1+1/\varepsilon_n} f_n^{1+1/\varepsilon_n} \right] \right)^{1-1/\psi} \right\}$$

³² In the following, we often skip the explicit dependence of μ_S and μ_K on their variables if this does not cause any confusion.

$$\begin{aligned}
& -\delta\theta J + J_t + J_{K_1}K_1\left(i_1 - \frac{1}{2}\phi_1 i_1^2 + r - \frac{1}{2}\kappa r^2 - \delta_1^k\right) + J_{K_2}K_2\left(i_2 - \frac{1}{2}\phi_2 i_2^2 - r\frac{K_1}{K_2} - \delta_2^k\right) \\
& + \frac{1}{2}J_{K_1K_1}K_1^2\sigma_1^2 + \frac{1}{2}J_{K_2K_2}K_2^2\sigma_2^2 + J_{K_1K_2}K_1K_2\sigma_1\sigma_2\rho_{12} + J_T\beta K_2 f_2 + J_{TT}\frac{1}{2}\sigma_T(T)^2 \\
& + \lambda_e\mathbb{E}[J(K_1(1-\ell_e), K_2(1-\ell_e), T) - J] + \lambda_c(T)\mathbb{E}[J(K_1(1-\ell_c), K_2(1-\ell_c), T) - J]\}.
\end{aligned}$$

We conjecture that the value function has the form

$$J(K_1, K_2, T) = \frac{1}{1-\gamma}(K_1 + K_2)^{1-\gamma}G(T, S(K_1, K_2)).$$

This specification implies

$$G(T, S) > 0 \quad \text{and} \quad G_T(T, S) > 0.$$

The partial derivatives of S are $S_{K_1} = \frac{-S}{K_1+K_2}$ and $S_{K_2} = \frac{1-S}{K_1+K_2}$. The relevant partial derivatives of the value function J are

$$\begin{aligned}
J_{K_1} &= K^{-\gamma}G + \frac{1}{1-\gamma}K^{1-\gamma}G_S\frac{-S}{K}, \\
J_{K_1K_1} &= -\gamma K^{-\gamma-1}G + 2K^{-\gamma}G_S\frac{-S}{K} + \frac{1}{1-\gamma}K^{1-\gamma}\left[G_{SS}\frac{S^2}{K^2} + 2G_S\frac{S}{K^2}\right], \\
J_{K_2} &= K^{-\gamma}G + \frac{1}{1-\gamma}K^{1-\gamma}G_S\frac{1-S}{K}, \\
J_{K_2K_2} &= -\gamma K^{-\gamma-1}G + 2K^{-\gamma}G_S\frac{1-S}{K} + \frac{1}{1-\gamma}K^{1-\gamma}\left[G_{SS}\frac{(1-S)^2}{K^2} - 2G_S\frac{1-S}{K^2}\right], \\
J_{K_1K_2} &= -\gamma K^{-1-\gamma}G + K^{-\gamma}G_S\frac{1-2S}{K} + \frac{1}{1-\gamma}K^{1-\gamma}\left[G_{SS}\frac{-(1-S)S}{K^2} + G_S\frac{2S-1}{K^2}\right], \\
J_T &= \frac{1}{1-\gamma}K^{1-\gamma}G_T.
\end{aligned}$$

Substituting the conjecture and its partial derivatives into the HJB equation leads to the following reduced-form HJB equation:

$$(A.10) \quad 0 = \sup_{i_1, i_2, f_1, f_2, r} \left\{ G_t + M_0 + M_1G + M_2G_S + M_3G_{SS} + M_4G_T + M_5G_{TT} \right\}.$$

We introduce the three-dimensional volatility vectors

$$(A.11) \quad \sigma_k(S) = \left((1-S)\sigma_1 + S\sigma_2\rho_{12}, S\sigma_2\sqrt{1-\rho_{12}^2}, 0 \right)^\top,$$

$$(A.12) \quad \sigma_s = \left(\sigma_2\rho_{12} - \sigma_1, \sigma_2\sqrt{1-\rho_{12}^2}, 0 \right)^\top.$$

The coefficients M_ℓ ($\ell = 1, \dots, 5$) are given by

$$\begin{aligned}
M_0 &= \delta\theta G^{1-1/\theta} c^{1-1/\psi}, \\
M_1 &= (1-\gamma) \left[\underbrace{(1-S)\mu_1 + S\mu_2}_{=\mu_k} - \frac{1}{2}\gamma \underbrace{[(1-S)^2\sigma_1^2 + S^2\sigma_2^2 + 2S(1-S)\sigma_1\sigma_2\rho_{12}]}_{=\|\sigma_k\|^2} \right] - \delta\theta \\
&\quad + \lambda_e\mathbb{E}[(1-\ell_e)^{1-\gamma} - 1] + \lambda_c(T)\mathbb{E}[(1-\ell_c)^{1-\gamma} - 1], \\
M_2 &= S(1-S) \left(\mu_2 - \mu_1 - \gamma \left[\underbrace{S\sigma_2^2 - (1-S)\sigma_1^2 + (1-2S)\sigma_1\sigma_2\rho_{12}}_{=\sigma_k^\top\sigma_s} \right] \right),
\end{aligned}$$

$$\begin{aligned}
M_3 &= \frac{1}{2}(1-S)^2 S^2 \left[\underbrace{\sigma_1^2 + \sigma_2^2 - 2\sigma_1\sigma_2\rho_{12}}_{=\|\sigma_s\|^2} \right], \\
M_4 &= \widehat{\beta} f_2, \quad \text{and} \quad M_5 = \frac{1}{2}\sigma_T(T)^2,
\end{aligned}$$

where c is given in (A.2) and $\widehat{\beta} = \beta/K_2$. The separation thus holds if and only if $\widehat{\beta}$ is independent of K_1 and K_2 , that is, $\widehat{\beta} = \widehat{\beta}(t, T, S)$. Calculating the first-order optimality conditions leads to the nonlinear system of Equations (A.4)–(A.8) that determines the optimal controls. This proves the proposition. \square

A.2. Stochastic Discount Factor (SDF). The information about the current value of future (uncertain) cash flows is summarized by the SDF or pricing kernel. If the SDF is known, we can calculate today's price of any given cash-flow stream. It generalizes standard discount factor ideas. Duffie and Epstein (1992a) and Duffie and Skiadas (1994) show that for continuous-time recursive utility the SDF has the form

$$(A.13) \quad H_s = \exp\left(\int_0^s f_J(C_u, J_u) du\right) f_C(C_s, J_s),$$

where J_s denotes the time- s value of the value function. Applying Ito's lemma to (A.13) gives

$$(A.14) \quad \frac{dH}{H_-} = \frac{df_C(C_-, J_-)}{f_C(C_-, J_-)} + f_J(C, J)dt,$$

where subscripts of f denote partial derivatives. These dynamics contain several pieces of relevant information about key variables of the economy. Its drift rate equals the equilibrium risk-free interest rate (with negative sign) and the coefficients in front of the Brownian shocks contain the market prices of diffusive risk, see Proposition A.2 below.

PROPOSITION A.2 (EQUILIBRIUM). *Let $\sigma_k(S_t)$ be the three-dimensional volatility vector of the total stock of capital, see (A.11), and $\sigma_g(t, S_t, T_t)$ the three-dimensional volatility vector of G , see (A.16). Let $\mu_C(t, S_t, T_t)$ and $\sigma_C(t, S_t, T_t)$ denote the drift rate and the three-dimensional volatility vector of aggregate consumption, respectively, see (A.18) and (A.19). The SDF follows the dynamics*

$$\frac{dH}{H_-} = -r^f dt + \Theta_W^\top dW + \sum_{i \in \{e, c\}} ((1 - \ell_i)^{-\gamma} - 1) dN_i - \Theta_N dt$$

with $W = (W_1, W_2, W_3)^\top$. The equilibrium risk-free rate r^f is

$$\begin{aligned}
r_t^f &= \underbrace{\delta + \frac{1}{\psi}\mu_C - \frac{1}{2}\gamma\left(1 + \frac{1}{\psi}\right)\|\sigma_C\|^2}_{\text{standard diffusion risk}} + \underbrace{\sum_{i \in \{e, c\}} \lambda_i(T)\mathbb{E}\left[(1 - \ell_i)^{-\gamma} - 1 - \frac{\psi^{-1} - \gamma}{1 - \gamma}(1 - (1 - \ell_i)^{1-\gamma})\right]}_{\text{disaster risk}} \\
&\quad + \underbrace{\frac{\gamma\psi - 1}{2\psi^2}(\|\sigma_C - \sigma_k\|^2 + \psi(\|\sigma_C\|^2 - \|\sigma_k\|^2)) + \frac{\theta - 1}{\psi\theta}\sigma_g^\top(\sigma_C - \sigma_k)}_{\text{temperature interaction risk}},
\end{aligned}$$

where $\|\cdot\|$ is the Euclidean norm. The market prices of diffusion risk and jump risk are

$$\Theta_{W_t} = \underbrace{-\gamma\sigma_C}_{\text{standard risk}} + \underbrace{\frac{\theta-1}{\theta}\sigma_g + \left(\gamma - \frac{1}{\psi}\right)(\sigma_C - \sigma_k)}_{\text{temperature risk}}, \quad \Theta_{N_t} = \sum_{i \in \{e,c\}} \lambda_i(T_t) \mathbb{E}[(1 - \ell_i)^{-\gamma} - 1].$$

A.3. *Proof of Proposition A.2.* We have

$$f_c(C, J) = \delta G^{1-1/\theta} K^{-\gamma} c^{-1/\psi} \quad \text{and} \quad f_J(C, J) = \delta(\theta - 1)c^{1-1/\psi} G^{-1/\theta} - \delta\theta.$$

To calculate the dynamics of the SDF, we first compute

$$\frac{dK^{-\gamma}}{K^{-\gamma}} = (-\gamma\mu_k + \frac{1}{2}\gamma(\gamma+1)\|\sigma_k\|^2)dt - \gamma\sigma_k^\top dW + \sum_{i \in \{e,c\}} ((1 - \ell_i)^{-\gamma} - 1)dN_i.$$

Next, we determine the dynamics of $G^{1-1/\theta}$. According to Itô's lemma, G satisfies

$$dG = G[\mu_g dt + \sigma_g^\top dW]$$

with

$$(A.15) \quad \mu_g = \frac{1}{G}(G_t + G_S S(1-S)\mu_s + G_T \beta f_2 + \frac{1}{2}G_{SS}S^2(1-S)^2\|\sigma_s\|^2 + \frac{1}{2}G_{TT}\sigma_T(T)^2),$$

$$(A.16) \quad \sigma_g = \frac{1}{G}(G_S S(1-S)(-\sigma_1 + \sigma_2 \rho_{12}), G_S S(1-S)\sigma_2 \sqrt{1 - \rho_{12}^2}, G_T \sigma_T(T))^\top.$$

Another application of Itô's lemma yields

$$\frac{dG^{1-1/\theta}}{G^{1-1/\theta}} = \left[\frac{\theta-1}{\theta}\mu_g - \frac{\theta-1}{2\theta^2}\|\sigma_g\|^2\right]dt + \frac{\theta-1}{\theta}\sigma_g^\top dW.$$

Therefore, by Itô's product rule,

$$(A.17) \quad \begin{aligned} \frac{d(G^{1-1/\theta}K^{-\gamma})}{(G^{1-1/\theta}K^{-\gamma})_-} &= \left(-\gamma\mu_k + \frac{1}{2}\gamma(\gamma+1)\|\sigma_k\|^2\right)dt + \frac{\theta-1}{\theta}(\mu_g - \gamma\langle\sigma_k, \sigma_g\rangle)dt \\ &\quad - \frac{\theta-1}{2\theta^2}\|\sigma_g\|^2dt + \left(\frac{\theta-1}{\theta}\sigma_g - \gamma\sigma_k\right)^\top dW + \sum_{i \in \{e,c\}} ((1 - \ell_i)^{-\gamma} - 1)dN_i. \end{aligned}$$

Notice that according to the simplified HJB equation (A.10),

$$\mu_g - \gamma\langle\sigma_k, \sigma_g\rangle \frac{G_S}{G} S(1-S) = (\gamma-1)(\mu_k - \frac{1}{2}\gamma\|\sigma_k\|^2) + \delta\theta - \delta\theta G^{-1/\theta} c^{1-1/\psi} - \sum_{i \in \{e,c\}} \lambda_i \mathbb{E}[(1 - \ell_i)^{1-\gamma} - 1].$$

Substituting this term into Equation (A.17) yields

$$\begin{aligned} \frac{d(G^{1-1/\theta}K^{-\gamma})}{(G^{1-1/\theta}K^{-\gamma})_-} &= (-\gamma\mu_k + \frac{1}{2}\gamma(\gamma+1)\|\sigma_k\|^2)dt - \frac{\theta-1}{2\theta^2}\|\sigma_g\|^2dt \\ &\quad + \frac{\theta-1}{\theta}((\gamma-1)(\mu_k - \frac{1}{2}\gamma\|\sigma_k\|^2) + \delta\theta - \delta\theta G^{-1/\theta} c^{1-1/\psi})dt + \left(\frac{\theta-1}{\theta}\sigma_g - \gamma\sigma_k\right)^\top dW \\ &\quad + \sum_{i \in \{e,c\}} ((1 - \ell_i)^{-\gamma} - 1)dN_i - \frac{\theta-1}{\theta} \sum_{i \in \{e,c\}} \lambda_i \mathbb{E}[(1 - \ell_i)^{1-\gamma} - 1]dt. \end{aligned}$$

The consumption-capital ratio $c = C/K$ has the following dynamics:

$$\frac{dc}{c} = \mu_c dt + \sigma_c^\top dW$$

for auxiliary functions $\mu_c(t, S, T)$ and $\sigma_c(t, S, T)$, which can be determined numerically (see Subsection B.2 of the online appendix). In turn,

$$\frac{dc^{-1/\psi}}{c^{-1/\psi}} = -\frac{1}{\psi}(\mu_c dt + \sigma_c^\top dW) + \frac{1+\psi}{2\psi^2} \|\sigma_c\|^2 dt.$$

Set $\tilde{H} = G^{1-1/\theta} K^{-\gamma}$. Then, $df_c(C, J) = \delta(\tilde{H}_- dc^{-1/\psi} + c_-^{-1/\psi} d\tilde{H} + d\langle c^{-1/\psi}, \tilde{H} \rangle)$. Consequently, the pricing kernel dynamics are given by

$$\begin{aligned} \frac{dH_-}{H_-} &= \frac{df_c}{f_c} + f_j dt \\ &= -\left(\delta + \frac{1}{\psi}\mu_k - \frac{1}{2}\gamma\left(1 + \frac{1}{\psi}\right)\|\sigma_k\|^2\right)dt - \frac{1}{\psi}\mu_c + \frac{1+\psi}{2\psi^2}\|\sigma_c\|^2 + \frac{\gamma}{\psi}\sigma_c^\top \sigma_k dt \\ &\quad - \left(\frac{\theta-1}{2\theta^2}\|\sigma_g\|^2 + \frac{\theta-1}{\psi\theta}\sigma_c^\top \sigma_g\right)dt + \left(-\gamma\sigma_k + \frac{\theta-1}{\theta}\sigma_g - \frac{1}{\psi}\sigma_c\right)^\top dW \\ &\quad + \sum_{i \in \{e, c\}} \lambda_i \mathbb{E} \left[(1 - \ell_i)^{-\gamma} - 1 + \frac{\psi^{-1}-\gamma}{1-\gamma} (1 - (1 - \ell_i)^{1-\gamma}) \right] dt \\ &\quad + \sum_{i \in \{e, c\}} \left[((1 - \ell_i)^{-\gamma} - 1) dN^i - \lambda_i \mathbb{E} [(1 - \ell_i)^{-\gamma} - 1] dt \right]. \end{aligned}$$

Another application of Itô's product rule yields the drift and volatility vector of optimal consumption

$$(A.18) \quad \mu_C(t, S, T) = \mu_C(S) + \mu_c(t, S, T) + \sigma_c(t, S, T)^\top \sigma_k(S),$$

$$(A.19) \quad \sigma_C(t, S, T) = \sigma_k(S) + \sigma_c(t, S, T).$$

Substituting Equations (A.18) and (A.19) into the pricing kernel dynamics and some algebra finishes the proof. \square

A.4. *Dividend Dynamics.* The amount of consumption goods produced in sector n are

$$C_n = Y_n - I_n - b_n F_n = c_n K_n$$

with $c_n = A_n f_n^{\eta_n} \Lambda_n(T) - i_n - \frac{b_n}{1+1/\varepsilon_n} f_n^{1+1/\varepsilon_n}$. Application of Ito's lemma shows that c_n evolves according to

$$\frac{dc_n}{c_n} = \mu_{c_n} dt + \sigma_{c_n}^\top dW$$

for auxiliary functions μ_{c_n}, σ_{c_n} that can be determined numerically along the lines of Subsection B.2 of the online appendix. Notice that c_n is unaffected when the economy is hit by a disaster shock N^d .

Empirically, dividends are more volatile than consumption (e.g., Bansal and Yaron, 2004) and dividends fall more than consumption when a disaster hits the economy (e.g., Longstaff and Piazzesi, 2004). Following Wachter (2013), among others, we thus model dividends as leveraged consumption, that is, $D_n = C_n^\varphi$ for $\varphi \geq 1$.³³ Application of Ito's product rule yields the dividend dynamics

$$(A.20) \quad \frac{dD_n}{D_n} = \mu_{D_n} dt + \sigma_{D_n}^\top dW + \sum_{i \in \{e, c\}} [(1 - \ell_i)^\varphi - 1] dN^i$$

³³ A popular alternative to this approach is modeling the consumption-dividend ratio as a stationary but persistent process, as in Longstaff and Piazzesi (2004), among others. To focus on the novel implications of climate risk on asset prices, we keep the setting simple. However, following this approach would also be feasible in our setting.

with

$$\begin{aligned}\mu_{D_n} &= \varphi(\mu_{K_n} + \mu_{c_n} + \sigma_{c_n}^\top \sigma_{K_n}) + \frac{1}{2}\varphi(\varphi - 1)\|\sigma_{k_n} + \sigma_{c_n}\|^2, \\ \sigma_{D_n} &= \varphi(\sigma_{k_n} + \sigma_{c_n}).\end{aligned}$$

In a second step, we determine the dynamics of discounted dividends, $\widehat{D}_n = HD_n$. Another application of Itô's product rule implies

$$\frac{d\widehat{D}_n}{\widehat{D}_n} = \mu_{\widehat{D}_n}(S, T)dt + \sigma_{\widehat{D}_n}(T, S)^\top dW + \sum_{i \in \{c, e\}} ((1 - \ell_i)^{\varphi - \gamma} - 1)dN_i$$

with

$$\mu_{\widehat{D}_n} = \mu_H + \mu_{D_n} + \Theta_H^\top \sigma_{D_n} \quad \text{and} \quad \sigma_{\widehat{D}_n} = \Theta_H + \sigma_{D_n}.$$

A.5. Price-Dividend Ratios of Dividend Claims. Let $\omega_n = \log(\frac{P_n}{D_n})$ denote the log of the price-dividend ratio of asset n . Due to the representation (A.20) of the dividends, the dynamics of K_n (1, 2), and the pricing equation

$$P_{nt} = \mathbb{E}_t \left[\int_t^\infty \frac{H_s}{H_t} \mathcal{D}_{ns} ds \right],$$

the price is linear in \mathcal{D}_n , and the price-dividend ratio is independent of K_n . Therefore, it is a continuous process with dynamics

$$\frac{d\omega_n}{\omega_n} = \mu_{\omega_n} dt + \sigma_{\omega_n}^\top dW,$$

where the drift and the volatility vector are given by

$$\begin{aligned}\mu_{\omega_n} &= \frac{1}{\omega_n} [\omega_{n,t} + \omega_{n,S} S(1 - S)\mu_S + \omega_{n,T} \mu_T + \frac{1}{2}\omega_{n,TT} \|\sigma_T\|^2 + \frac{1}{2}\omega_{n,SS} S^2(1 - S)^2 \|\sigma_S\|^2] \\ \sigma_{\omega_n} &= \frac{1}{\omega_n} [\omega_{n,T} \sigma_T + \omega_{n,S} S(1 - S)\sigma_S].\end{aligned}$$

In particular, the price-dividend ratio $\Omega_n = e^{\omega_n}$ satisfies the following dynamics:

$$\frac{d\Omega_n}{\Omega_n} = \left(\omega_n \mu_{\omega_n} + \frac{1}{2} \omega_n^2 \|\sigma_{\omega_n}\|^2 \right) dt + \omega_n \sigma_{\omega_n}^\top dW.$$

We rewrite the discounted asset price HP_n as $F_n(\widehat{D}_n, \omega_n) = \widehat{D}_n e^{\omega_n}$. It follows from Itô's lemma that

$$\frac{dF_n}{F_n} = (\mu_{\widehat{D}_n} + \omega_n \mu_{\omega_n} + \frac{1}{2} \omega_n^2 \|\sigma_{\omega_n}\|^2 + \omega_n \sigma_{\omega_n}^\top \sigma_{\widehat{D}_n}) dt + (\omega_n \sigma_{\omega_n} + \sigma_{\widehat{D}_n})^\top dW + \sum_{i \in \{e, c\}} ((1 - \ell_i)^{\varphi - \gamma} - 1) dN_i.$$

An application of the Feynman–Kač Theorem yields

$$(A.21) \quad \mathcal{L}F_n + e^{-\omega_n} F_n = 0,$$

where $\mathcal{L}F_n$ denotes the infinitesimal generator. The no-arbitrage condition implies

$$(A.22) \quad \frac{\mathcal{L}F_n}{F_n} = \mu_{\widehat{D}_n} + \omega_n \mu_{\omega_n} + \frac{1}{2} \omega_n^2 \|\sigma_{\omega_n}\|^2 + \omega_n \sigma_{\omega_n}^\top \sigma_{\widehat{D}_n} + \sum_{i \in \{e, c\}} \lambda_i \mathbb{E}[(1 - \ell_i)^{\varphi - \gamma} - 1].$$

Substituting (A.22) into (A.21) yields

$$0 = \mu_{\widehat{D}_n} + \omega_n \mu_{\omega_n} + \frac{1}{2} \omega_n^2 \|\sigma_{\omega_n}\|^2 + \omega_n \sigma_{\omega_n}^\top \sigma_{\widehat{D}_n} + \lambda_d \sum_{i \in \{e, c\}} \lambda_i \mathbb{E}[(1 - \ell_i)^{\varphi - \gamma} - 1] + e^{-\omega_n}.$$

Consequently, we obtain the following partial differential equation (PDE) for the log of the price-dividend ratio ω_n :

$$\begin{aligned} 0 = & \sum_{i \in \{e, c\}} \lambda_i \mathbb{E}[(1 - \ell_i)^{\phi - \gamma} - 1] + e^{-\omega_n} + \mu_{\widehat{D}_n} + \omega_{n,t} + \omega_{n,S} S(1 - S)\mu_S + \omega_{n,T} \mu_T \\ & + \frac{1}{2}(\omega_{n,TT} + \omega_{n,T}^2) \|\sigma_T\|^2 + \frac{1}{2}(\omega_{n,SS} + \omega_{n,S}^2) S^2(1 - S)^2 \|\sigma_S\|^2 \\ & + (\omega_{n,TS} + \omega_{n,S} S(1 - S)\sigma_S)^\top \sigma_{\widehat{D}_n}. \end{aligned}$$

Notice that this PDE is nonlinear since it involves squared partial derivatives of ω_n . To simplify the numerical solution approach, we transform this PDE into a linear, parabolic PDE that can be solved using finite differences. We substitute $\Omega_n = e^{\omega_n}$ and end up with

$$\begin{aligned} (A.23) \quad 0 = & 1 + \Omega_n(\mu_{\widehat{D}_n} + \lambda_d \mathbb{E}[(1 - \ell)^{1 - \gamma} - 1]) + \Omega_{n,t} + \Omega_{n,S} S(1 - S)\mu_S + \Omega_{n,T} \mu_T + \frac{1}{2} \Omega_{n,TT} \|\sigma_T\|^2 \\ & + \frac{1}{2} \Omega_{n,SS} S^2(1 - S)^2 \|\sigma_S\|^2 + (\Omega_{n,TS} + \Omega_{n,S} S(1 - S)\sigma_S)^\top \sigma_{\widehat{D}_n}. \end{aligned}$$

A.6. *Risk Premia.* The dynamics of the asset price $P_n = e^{\omega_n} D_n$ follow via Itô's lemma:

$$\frac{dP_n}{P_n} = \mu_{P_n} dt + \sigma_{P_n}^\top dW + \sum_{i \in \{c, e\}} [(1 - \ell_i)^\varphi - 1] dN_i - \sum_{i \in \{c, e\}} \lambda_i \mathbb{E}[(1 - \ell_i)^\varphi - 1] dt,$$

where the expected stock return and the volatility vector are given by

$$\begin{aligned} \mu_{P_n} &= \mu_{\omega_n} + \mu_{D_n} + \sigma_{D_n}^\top \sigma_{\omega_n} + \frac{1}{2} \|\sigma_{\omega_n}\|^2 + \sum_{i \in \{c, e\}} \lambda_i \mathbb{E}[(1 - \ell_i)^\varphi - 1], \\ \sigma_{P_n} &= \sigma_{\omega_n} + \sigma_{D_n}. \end{aligned}$$

Now, the risk premium of asset n can be computed as the sum of its expected stock return, μ_{P_n} , and its dividend yield, $e^{-\omega_n}$, minus the risk-free interest rate, r^f , that is,

$$\text{rp}_n = \mu_{P_n} + e^{-\omega_n} - r^f.$$

A.7. *Further Details of the Calibration.*

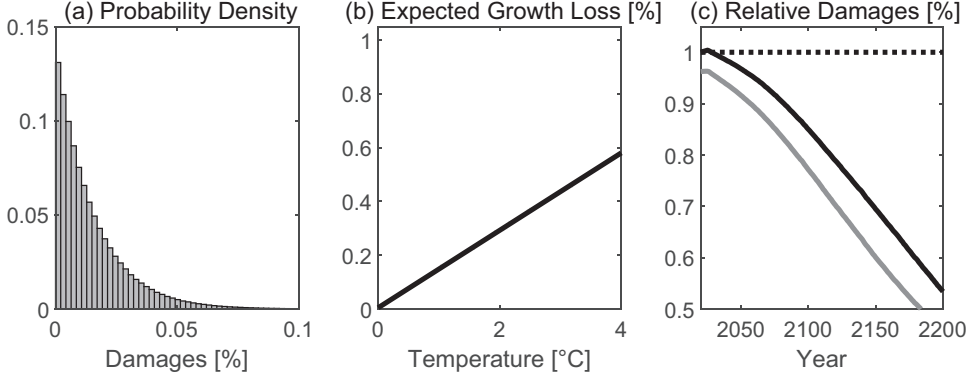
Economic Model For our calibration, we follow Pindyck and Wang (2013). Their model only involves a single capital stock and abstracts from climate change, but it can be nested in our two-sector model. The model is well-suited to explain *historical* asset returns, since brown capital has dominated the world economy in the past, but the influence of climate change on asset markets is almost negligible. In the long run, there might be a transition from brown to green capital. Yet, the current share of green capital is only about 6% indicating that the transition to green energy has been very modest.³⁴ We consider the special case of our model with only one capital stock and assume that it evolves as

$$dK = \left(I - \frac{1}{2} \phi \frac{I^2}{K} - \delta_k K \right) dt + K \sigma dW_1 - K \ell_e dN_e,$$

where output is $Y = AK^{1-\eta} F^\eta = I + C + \frac{b}{1+1/\varepsilon} F^{1+1/\varepsilon} K^{-1/\varepsilon}$. In the social optimum, the model collapses to a linear AK production function $Y = A^* K$ with productivity

$$(A.24) \quad A^* = A \left(\frac{b}{\eta A} \right)^{\frac{\eta}{\eta-1-1/\varepsilon}}.$$

³⁴ See the Web site of the United Nations Framework Convention on Climate Change (UNFCCC), <https://unfccc.int/news/green-economy-overtaking-fossil-fuel-industry-ftse-russel-report>.



NOTES: Panel (a) depicts the histogram of the annual damage distribution conditioned on being hit by a climate disaster from the EM-DAT database. Panel (b) relates the expected annual loss of economic growth, $\lambda_c(T)\mathbb{E}[\ell_c]$, to temperature. Panel (c) depicts the median relative damages in models with level (TFP) impact as in the DICE model and with disaster impact expressed in terms of consumption (gray line) and output (black line) in the BAU scenario. The black line depicts the median evolution of $1 - Y_t^{\text{BAU, disaster}}/Y_t^{\text{BAU, dice}}$ and the gray line depicts the median evolution of $1 - C_t^{\text{BAU, disaster}}/C_t^{\text{BAU, dice}}$.

FIGURE A.1

CALIBRATION OF CLIMATE DISASTER IMPACT

The one-sector model is similar to that of Pindyck and Wang (2013), but involves an energy input F , which does not cause climate change. We fix the dividend leverage parameter at $\varphi = 2.8$ (cf. Bansal and Yaron, 2004). We choose a time-preference rate of $\delta = 0.015$ per year, which is standard in the literature on optimal carbon pricing (e.g., Nordhaus, 2017). We set the energy shares to $\eta_i = 0.066$ (cf. van den Bremer and van der Ploeg, 2021).

We calibrate the remaining parameters of this one-sector model such that it generates a real expected growth rate of consumption of $\bar{\mu}_c = 2\%$, an average consumption rate of $\chi = \frac{C}{A^*K} = 75\%$ of GDP, an annual risk-free interest rate starting at $r^f = 0.8\%$, an average risk premium of $\text{rp} = 6.6\%$, and Tobin's Q's of $q = 1.548$. The following equations constitute a nonlinear system that relates ψ , γ , A^* , ϕ , and φ to the quantities

$$(A.25) \quad \chi = \frac{q}{A^*} \left[\delta + \left(\frac{1}{\psi} - 1 \right) \left(\bar{\mu} - 0.5\gamma\sigma^2 - \frac{\lambda_d}{\alpha - \gamma + 1} \right) \right],$$

$$(A.26) \quad \bar{\mu}_c = -\delta_k + A \left(1 - \chi - \frac{\eta}{1+1/\varepsilon} \right) - \frac{1}{2} \phi A^2 \left(1 - \chi - \frac{\eta}{1+1/\varepsilon} \right)^2 - \frac{\lambda_e}{\alpha_e + 1},$$

$$(A.27) \quad r^f = \delta + \frac{\bar{\mu}_c}{\psi} - \frac{1}{2} \gamma \left(1 + \frac{1}{\psi} \right) \sigma_c^2 - \lambda_e \frac{\left(\frac{1}{\psi} - \gamma \right) (\alpha_e - \gamma) + \gamma (\alpha_e - \gamma + 1)}{(\alpha_e - \gamma) (\alpha_e - \gamma + 1)},$$

$$(A.28) \quad \text{rp} = \varphi \gamma \sigma_c^2 + \lambda_e \gamma \left[\frac{1}{\alpha_e - \gamma} - \frac{\alpha_e}{(\alpha_e + \varphi) (\alpha_e - \gamma + \varphi)} \right],$$

$$(A.29) \quad q = \frac{1}{1 - \phi i}.$$

For the derivation of these equations and further details, we refer to Pindyck and Wang (2013). Finally, we back out the total factor productivity A from Equation (A.24).

Next, we calibrate the cost parameters b_1 and b_2 . We use an average global cost of fossil fuel 540 USD per ton of carbon (cf. van den Bremer and van der Ploeg, 2021) and a significantly higher average global price of green energy, that is, 810 USD for the same amount of energy, which is in line with production costs in developed countries such as Germany. The optimal solution to this one-sector model implies that the aggregate costs of energy are given

by

$$(A.30) \quad \frac{b}{1 + 1/\varepsilon} \left(\frac{Y}{A^*} \right)^{-1/\varepsilon} F^{1+1/\varepsilon} = \frac{\eta Y}{1 + 1/\varepsilon}.$$

Given the average values \bar{b} , the optimal BAU-energy use must satisfy $F = \frac{\eta Y}{\bar{b}(1+1/\varepsilon)}$. Hence, Equation (A.30) determines the cost parameter b .

Climate Disasters Figure A.1 depicts the calibration of climate disasters. Panel (a) shows the distribution of climate damages if a climate disaster hits the economy. Panel (b) shows the expected annual loss of economic growth in response to higher temperatures, $\lambda_c(T)\mathbb{E}[\ell_c]$. Panel (c) shows the relative impact of climate disasters compared to the Nordhaus level damage. Due to the persistent impact on economic growth and the potentially high magnitude of damages, the disaster impact causes much more severe climate damages than the Nordhaus specification, and its severity is more in line with recent evidence (e.g., Burke et al., 2015).³⁵

SUPPORTING INFORMATION

Additional supporting information may be found online in the Supporting Information section at the end of the article.

Figure A.1: Policy Functions with Level Impact of Climate Change as function of S and T.

Figure A.2: Asset Pricing without Option to Convert as function of S and T.

Table A.1: Decomposition of the Risk-free Rate for the Year 2100.

Figure A.3: Asset Pricing versus Temperature and the Share of Brown Capital (Climate Disasters).

Figure A.4: Evolution of Temperature, the Social Cost of Carbon and the Real Economy.

Figure A.5: Evolution of Tobin's Q's, Risk-Free Rates and the Risk Premia.

Figure A.6: Sample Paths of Green and Brown Returns.

Figure A.7: Abatement and Diversification Motives with Climate Disasters.

Figure A.8: Abatement and Diversification Motives with Unleveraged Dividends.

Figure A.9: Time Paths for the Optimal Carbon Taxes.

Figure A.10: Abatement and Diversification Motives with Accelerated Green Transition Driven by Directed Technological Change: Faster Cost Reductions Based on Solar Power Experience.

Figure A.11: Heterogeneous Volatilities.

Figure A.12: Higher and Lower Different Instantaneous Volatilities.

Figure A.13: Positive and Negative Different Instantaneous Correlations

Figure A.14: Imperfectly Substitutable Final Goods.

Figure A.15: Changes in the Reallocation Cost Parameter

Figure A.16: Lower Total Factor Productivity for the Green Sector.

Figure A.17: Increasing Intensities of Global Warming Damages.

Table A.2: Different Intensities for the Specifications of Global Warming Damages.

Figure A.18: Combining Different Types of Climate Damage Specifications.

Figure A.19: Brown Portfolio Shares for Different Instantaneous Correlations.

REFERENCES

ACEMOGLU, D., P. AGHION, L. BURSZTYN, and D. HEMOUS, "The Environment and Directed Technical Change," *American Economic Review* 102 (2012), 131–66.

³⁵ Results for other damage specifications (i.e., the Weitzman (2012) damage or growth rate impacts akin to Dell et al. (2009, 2012)) are available upon request.

- ACKERMAN, F., E. A. STANTON, and R. BUENO, "Epstein-Zin Utility in DICE: Is Risk Aversion Irrelevant to Climate Policy?," *Environmental and Resource Economics* 56 (2013), 73–84.
- ALLEN, M. R., D. J. FRAME, C. HUNTINGFORD, C. D. JONES, J. A. LOWE, M. MEINSHAUSEN, and N. MEINSHAUSEN, "Warming Caused by Cumulative Carbon Emissions towards the Trillionth Tonne," *Nature* 458 (2009), 1163–66.
- ARDIA, D., K. BLUTEAU, K. BOUDT, and K. INGHELBRECHT, "Climate Change Concerns and the Performance of Green vs. Brown Stocks," *Management Science* 69 (2023), 7151–882.
- ASWANI, J., A. RAGHUNANDAN, and S. RAJGOPAL, "Are Carbon Emissions Associated with Stock Returns?," *Review of Finance*, 28 (2024), 75–106.
- BANSAL, R., D. KIKU, and M. OCHOA, "Price of Long-Run Temperature Shifts in Capital Markets," Working Paper, Duke University, 2017.
- , ———, and ———, "Climate Change and Growth Risks," Working Paper, Duke University, 2019.
- , and A. YARON, "Risks for the Long Run: A Potential Resolution of Asset Pricing Puzzles," *Journal of Finance* 59 (2004), 1481–509.
- BARNETT, M., "Climate Change and Uncertainty: An Asset Pricing Perspective," *Management Science*, 69 (2023a), 7562–84.
- , "A Run on Fossil Fuel? Climate Change and Transition Risk," Working Paper, Arizona State University, 2023b.
- , W. BROCK, and L. P. HANSEN, "Pricing Uncertainty Induced by Climate Change," *Review of Financial Studies* 33 (2020), 1024–66.
- BARRO, R. J., "Rare Disasters and Asset Markets in the Twentieth Century," *Quarterly Journal of Economics* 121 (2006), 823–66.
- , "Rare Disasters, Asset Prices, and Welfare Costs," *American Economic Review* 99 (2009), 243–64.
- , and T. JIN, "On the Size Distribution of Macroeconomic Disasters," *Econometrica* 79 (2011), 1567–89.
- BAUER, M. D., D. HUBER, G. D. RUDEBUSCH, and O. WILMS, "Where is the Carbon Premium? Global Performance of Green and Brown Stocks," *Journal of Climate Finance* 1 (2022), 100006.
- BOLTON, P., and M. KACPERCZYK, "Do Investors Care about Carbon Risk?," *Journal of Financial Economics* 142 (2021), 517–49.
- , and ———, "Global Pricing of Carbon-Transition Risk," *Journal of Finance*, 78 (2023), 3677–754.
- BOVENBERG, A. L., and S. A. SMULDERS, "Transitional Impacts of Environmental Policy in an Endogenous Growth Model," *International Economic Review* 37 (1996), 861–93.
- BRETSCHGER, L., and A. VINOGRADOVA, "Best Policy Response to Environmental Shocks: Building a Stochastic Framework," *Journal of Environmental Economics and Management* 97 (2019), 23–41.
- BURKE, M., S. M. HSIANG, and E. MIGUEL, "Global Non-Linear Effect of Temperature on Economic Production," *Nature* 527 (2015), 235–39.
- CAI, Y., and T. S. LONTZEK, "The Social Cost of Carbon with Economic and Climate Risks," *Journal of Political Economy* 127 (2019), 2684–734.
- CASEY, G., "Energy Efficiency and Directed Technical Change: Implications for Climate Change Mitigation," *Review of Economic Studies* 91 (2024), 192–228.
- COCHRANE, J. H., F. A. LONGSTAFF, and P. SANTA-CLARA, "Two Trees," *Review of Financial Studies* 21 (2007), 347–85.
- CROST, B., and C. P. TRAEGER, "Optimal CO₂ Mitigation under Damage Risk Valuation," *Nature Climate Change* 4 (2014), 631–36.
- DANIEL, K., R. LITTERMAN, and G. WAGNER, "Declining CO₂ price paths," *Proceedings of the National Academy of Sciences of the United States of America* 116 (2019), 20886–91.
- DE LA TOUR, A., M. GLACHANT, and Y. MÉNIÈRE, "Predicting the Costs of Photovoltaic Solar Modules in 2020 Using Experience Curve Models," *Energy* 62 (2013), 341–48.
- DELL, M., B. F. JONES, and B. A. OLKEN, "Temperature and Income: Reconciling New Cross-Sectional and Panel Estimates," *American Economic Review* 99 (2009), 198–204.
- , ———, and ———, "Temperature Shocks and Economic Growth: Evidence from the Last Half Century," *American Economic Journal: Macroeconomics* 4 (2012), 66–95.
- DIETZ, S., C. GOLLIER, and L. KESSLER, "The Climate Beta," *Journal of Environmental Economics and Management* 87 (2018), 258–74.
- , and F. VENMANS, "Cumulative Carbon Emissions and Economic Policy: In Search of General Principles," *Journal of Environmental Economics and Management* 96 (2019), 108–29.
- DONADELLI, M., M. JUEPPNER, M. RIEDEL, and C. SCHLAG, "Temperature Shocks and Welfare Costs," *Journal of Economic Dynamics and Control* 82 (2017), 331–55.
- DUFFIE, D., and L. G. EPSTEIN, "Asset Pricing with Stochastic Differential Utility," *Review of Financial Studies* 5 (1992a), 411–36.

- , and ———, “Stochastic Differential Utility,” *Econometrica* 60 (1992b), 353–94.
- , and C. SKIADAS, “Continuous-Time Asset Pricing: A Utility Gradient Approach,” *Journal of Mathematical Economics* 23 (1994), 107–32.
- EL GHOUL, S., A. KAROUI, S. PATEL, and S. RAMANI, “The Green and Brown Performances of Mutual Fund Portfolios,” *Journal of Cleaner Production* 384 (2023), 135267.
- EPSTEIN, L. G., and S. E. ZIN, “Substitution, Risk Aversion, and the Temporal Behavior of Consumption and Asset Returns: A Theoretical Framework,” *Econometrica* 57 (1989), 937–69.
- GOLOSOV, M., J. HASSLER, P. KRUSELL, and A. TSYVINSKY, “Optimal Taxes on Fossil Fuel in General Equilibrium,” *Econometrica* 82 (2014), 41–88.
- HAMBEL, C., H. KRAFT, and E. S. SCHWARTZ, “Optimal Carbon Abatement in a Stochastic Equilibrium Model with Climate Change,” *European Economic Review* 132 (2021a), 103642.
- , ———, and ———, “The Social Cost of Carbon in a Non-cooperative World,” *Journal of International Economics* 131 (2021b), 103490.
- HSU, P.-H., K. LI, and C.-Y. TSOU, “The Pollution Premium,” *Journal of Finance* 78 (2023), 1343–92.
- IEA, *World Energy Outlook, 2021* (International Energy Agency, Paris, France, 2021).
- IPCC, *Fifth Assessment Report of the Intergovernmental Panel on Climate Change* (Cambridge University Press, Cambridge, United Kingdom, 2014).
- JENSEN, S., and C. P. TRAEGER, “Optimal Climate Change Mitigation under Long-Term Growth Uncertainty: Stochastic Integrated Assessment and Analytic Findings,” *European Economic Review* 69 (2014), 104–25.
- KARYDAS, C., and A. XEPAPADEAS, “Climate Change Financial Risks: Implications for Asset Pricing and Interest Rates,” *Journal of Financial Stability* 63 (2022), 101061.
- KREPS, D. M., and E. L. PORTEUS, “Temporal Resolution of Uncertainty and Dynamic Choice Theory,” *Econometrica* 46 (1978), 185–200.
- KUANG, W., “Are Clean Energy Assets a Safe Haven for International Equity Markets?,” *Journal of Cleaner Production* 302 (2021a), 127006.
- , “Which Clean Energy Sectors are Attractive? A Portfolio Diversification Perspective,” *Energy Economics* 104 (2021b), 105644.
- LEMOINE, D., “The Climate Risk Premium: How Uncertainty Affects the Social Cost of Carbon,” *Journal of the Association of Environmental and Resource Economists* 8 (2021), 27–57.
- LOAYZA, N. V., E. OLABERRA, J. RIGOLINI, and L. CHRISTIAENSEN, “Natural Disasters and Growth: Going Beyond the Averages,” *World Development* 40 (2012), 1317–36.
- LONGSTAFF, F. A., and M. PIAZZESI, “Corporate Earnings and the Equity Premium,” *Journal of Financial Economics* 74 (2004), 401–21.
- MARKOWITZ, H., “Portfolio Selection,” *Journal of Finance* 7 (1952), 77–91.
- MATTHEWS, H. D., N. P. GILLET, P. A. STOTT, and K. ZICKFELD, “The Proportionality of Global Warming to Cumulative Carbon Emissions,” *Nature* 459 (2009), 829–32.
- , K. ZICKFELD, R. KNUTTI, and M. R. ALLEN, “Focus on Cumulative Emissions, Global Carbon Budgets and the Implications for Climate Mitigation Targets,” *Environmental Research Letters* 13 (2018), 010201.
- MCGLADE, C., and P. EKINS, “The Geographical Distribution of Fossil Fuels Unused When Limiting Global Warming to 2° C,” *Nature* 517 (2015), 187–90.
- NORDHAUS, W. D., “To Slow or Not to Slow: The Economics of the Greenhouse Effect,” *Economic Journal* 101 (1991), 920–37.
- , “An Optimal Transition Path for Controlling Greenhouse Gases,” *Science* 258 (1992), 1315–19.
- , “Revisiting the Social Cost of Carbon,” *Proceedings of the National Academy of Sciences* 114 (2017), 1518–23.
- , and P. SZTORC, “DICE 2013R: Introduction and User’s Manual,” Technical Report, Yale University, 2013.
- PASTOR, L., R. F. STAMBAUGH, and L. A. TAYLOR, “Sustainable Investing in Equilibrium,” *Journal of Financial Economics* 142 (2021), 550–71.
- , ———, and ———, “Dissecting Green Returns,” *Journal of Financial Economics* 146 (2022), 403–24.
- PINDYCK, R. S., and N. WANG, “The Economic and Policy Consequences of Catastrophes,” *American Economic Journal: Economic Policy* 5 (2013), 306–39.
- PNG, I., *Managerial Economics* (Blackwell, Oxford, United Kingdom, 1999).
- REBOREDO, J. C., “Green Bond and Financial Markets: Co-Movement, Diversification and Price Spillover Effects,” *Energy Economics* 74 (2018), 38–50.
- , and A. UGOLINI, “Price Connectedness between Green Bond and Financial Markets,” *Economic Modelling* 88 (2020), 25–38.
- REZAI, A., and F. VAN DER PLOEG, “Intergenerational Inequality Aversion, Growth and the Role of Damages: Occam’s Rule for the Global Carbon Tax,” *Journal of the Association of Environmental and Resource Economists* 3 (2016), 499–522.

- SCHEFFERS, B., L. DE MEESTER, T. BRIDGE, A. HOFFMANN, J. PANDOLFI, R. CORLETT, S. BUTCHART, P. PEARCE-KELLY, K. KOVACS, D. DUDGEON, M. PACIFICI, C. RONDININI, W. FODEN, T. MARTIN, C. MORA, D. BICKFORD, and J. WATSON, "The Broad Footprint of Climate Change from Genes to Biomes to People," *Science* 354 (2019), 719–32.
- TRAEGER, C. P., "ACE—Analytic Climate Economy," *American Economic Journal: Economic Policy* 15 (2023), 372–406.
- VAN DEN BREMER, T. S., and F. VAN DER PLOEG, "The Risk-Adjusted Carbon Price," *American Economic Review*, 111 (2021), 2782–810.
- VAN DER PLOEG, F., "The Safe Carbon Budget," *Climatic Change* 147 (2018), 47–59.
- , and A. REZAI, "Stranded Assets in the Transition to a Carbon-Free Economy," *Annual Review of Resource Economics* 12 (2020), 1–18.
- WACHTER, J. A., "Can Time-Varying Risk of Rare Disasters Explain Aggregate Stock Market Volatility?," *Journal of Finance* 68 (2013), 987–1035.
- WEITZMAN, M. L., "GHG Targets as Insurance against Catastrophic Climate Damages," *Journal of Public Economic Theory* 14 (2012), 221–44.
- ZHANG, S., "Carbon Returns across the Globe," *Journal of Finance*, forthcoming, 2024.